

**Università degli Studi di Padova**

Dipartimento di Biologia

Corso di Laurea Magistrale in Biotecnologie Industriali



Production of polyhydroxyalkanoates by *Cupriavidus necator* in  
response to physiological stress for CO<sub>2</sub> capture

Relatore: Dr.ssa Laura Treu

Dipartimento di Biologia (DiBio)

Correlatore: Dr.ssa Rebecca Serna Garcia

Departament d'Enginyeria Química, Universitat de València

Controrelatore: Prof.ssa Elisabetta Schievano

Dipartimento di Scienze Chimiche (DiSC)

Laureando: Filippo Savio

Anno Accademico 2022/2023



# INDEX

<b>ABSTRACT</b>	<b>4</b>
<b>1. Introduction</b>	<b>5</b>
1.1. Polyhydroxyalkanoates: Shaping Sustainable Plastic Alternatives	6
1.2. Poly(3-hydroxybutyrate): Properties, Challenges, and Potential	7
1.3. <i>Cupriavidus necator</i> as a versatile organism for PHB production	9
1.4. Metabolic overview	10
1.5. Poly(3-hydroxybutyrate) production in <i>C.necator</i>	12
1.4. Aim of the thesis	13
<b>2. Materials and Methods</b>	<b>15</b>
2.1. Bacterial strain and inoculum preparation	15
2.2. Culture set-up and media preparation	15
2.3. CO <sub>2</sub> adaptation of maintenance culture	16
2.4. Analytical methods	17
2.5. Alternative carbon sources experiment set-up	17
2.6. Nitrogen and phosphorus starvation media	19
2.6.1. Heterotrophic N and P starvation	19
2.6.2. Autotrophic N starvation	19
2.6.3. Nile-Red staining	20
2.7. Transcriptomic experiment	21
2.7.1. Culture preparation and maintenance	21
2.7.2. RNA extraction and sequencing	22
2.8. PHA extraction and analysis	22
2.9. Gene expression analyses	23
<b>3. Results and discussion</b>	<b>24</b>
3.1. Adaptation from heterotrophic to chemolithotrophic metabolism	24
3.2. Exploration of carbon sources economically favourable	26
3.2.1. Growth analysis on volatile fatty acids	26
3.2.2. Growth analysis on acetic acid	28
3.3. Nutrients starvation trials	30
3.3.1. Heterotrophic growth trends during nitrogen and phosphorus starvation	30
3.3.2. Autotrophic growth trends during nitrogen starvation	32
3.4. Metabolic changes in <i>C. necator</i> upon chemolithotrophic growth	34
3.4.1. Comparison between adapted and not adapted conditions	34
3.4.2. Adaptation phase – PHB accumulation analysis	35
3.4.3. Overview of transcriptional profiles	36
<b>4. Conclusions</b>	<b>41</b>
<b>5. References</b>	<b>43</b>
<b>6. Appendix</b>	<b>52</b>

6.1. Appendix A - medium 81 recipe	52
6.2. Appendix B - VFA content	53
6.3. Appendix C - N starvation	55
6.4. Appendix D - PHB	55
6.5. Appendix E - Genes table	56

## ABSTRACT

The facultative chemolithotroph *Cupriavidus necator* exhibits a unique ability to thrive aerobically using both organic compounds in a heterotrophic way and hydrogen/carbon dioxide through chemolithotrophic way, concurrently accumulating polyhydroxybutyrate (PHB), a notable biopolymer classified under polyhydroxyalkanoates. This comprehensive investigation delves into the versatile growth dynamics of *C. necator* across diverse conditions, encompassing the utilisation of atmospheric carbon dioxide. The intricate interplay of carbon dioxide, hydrogen, and oxygen consumption and their impacts on microbial growth and PHB accumulation were monitored.

Furthermore, the bacterium's response to varying concentrations of volatile fatty acids as organic substrates was examined. The findings unveil the exceptional metabolic adaptability of *C. necator* under diverse conditions. In a bid to enhance PHB accumulation, the induction of nutritional stress, particularly through nitrogen and phosphorus deficiency, was explored within bacterial cells.

A comparative transcriptomic analysis sheds light on two distinct growth states of *C. necator*. One encompasses the adaptation to chemolithotrophic metabolism employing carbon dioxide, while the other involves the ongoing process of adaptation to carbon dioxide-reliant metabolism. This analysis unveils alterations in gene expression associated with distinct phases of adaptation, potentially intertwining with PHB synthesis pathways.

Collectively, this study illuminates *C. necator's* remarkable prowess in navigating a spectrum of growth conditions, accentuating its metabolic versatility. The exploration of genetic responses in respect with PHB synthesis open avenues for comprehending the molecular underpinnings of microbial adaptive mechanisms. Such insights hold promise for applications in sustainable biopolymer production and biotechnological advancements.

## 1. Introduction

Growing awareness of the environmental impact of industrial activities has sparked increasing interest in developing sustainable and innovative solutions to address the pressing challenges of reducing carbon dioxide (CO<sub>2</sub>) emissions and responsibly managing the plastic waste that plagues our planet. The need to redesign production processes and adopt eco-friendly approaches has proven urgent; this has led to an increasing search for alternatives to the intensive use of materials derived from fossil fuels. The European project "Harnessing potential of biological CO<sub>2</sub> capture for Circular Economy" (CooCE) aims to accelerate the development and upscale of biotechnological platforms for converting CO<sub>2</sub> into high-value market products (Fig. 1).

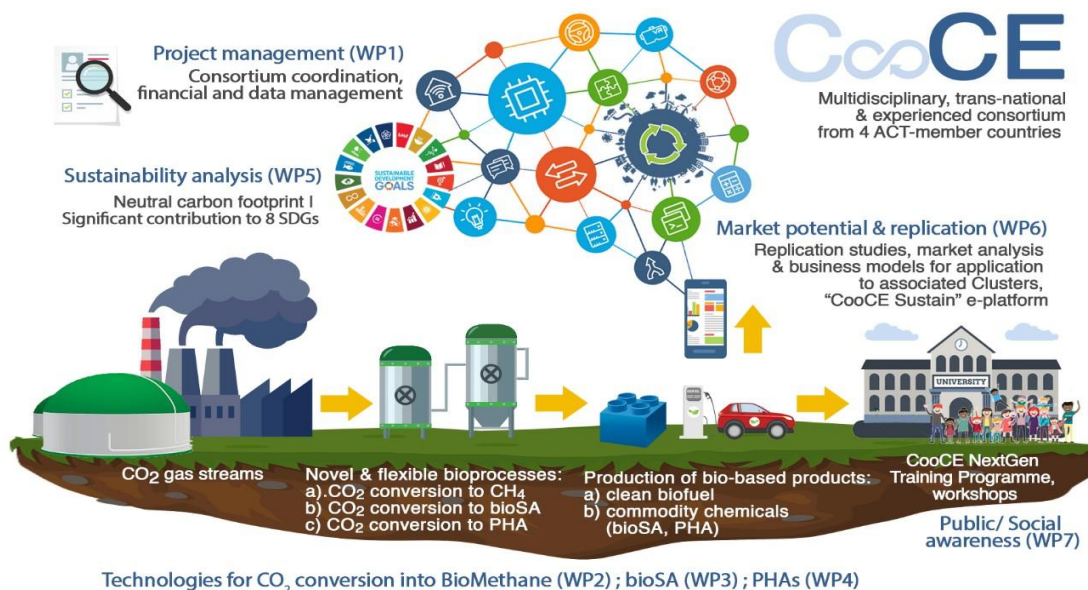


**Figure 1.** Technologies for CO<sub>2</sub> conversion into PHA and other high-value market products

In this evolving scenario, polyhydroxyalkanoates (PHA) are emerging as a promising class of biopolymers that play a key role in achieving the many ecological and

industrial goals facing modern society. PHA, aliphatic polymers synthesised by microorganisms through biological processes, are gaining increasing attention due to their exceptional properties and versatility in a wide range of industrial applications. Their ability to store carbon (C) in the form of intracellular granules makes them energy reserves within the cells themselves, suggesting new pathways toward the production of sustainable materials.

The prospect of obtaining bioplastics and polymeric materials through green metabolic pathways, based on renewable sources and processes with reduced environmental impact, proves attractive in a context where sustainability is at the centre of the global agenda. The environmental friendliness of PHA, their biodegradability, and the ability to modulate their chemical and physical properties make them ideal candidates to replace traditional plastics that pose a threat to the environment and biodiversity.

### 1.1. Polyhydroxyalkanoates: Shaping Sustainable Plastic Alternatives

PHA constitute a class of aliphatic polyesters that are synthesised and accumulated within microbial cells in intracellular granules. These polymers serve as C and energy stores, and their biosynthesis occurs in response to conditions of abundant C sources, often in conjunction with deficiency of specific nutrients. The heterogeneity of these compounds is associated with the C chain length of the constituent monomers: short-chain (SCL) polymers with 3-5 C atoms and medium-chain (MCL) polymers with 6-14 C atoms (Steinbüchel et al. 1992). In addition, PHA exhibit structural variations related to R side groups (**Fig. 2**), which can be branched or linear, saturated or unsaturated, leading to a wide diversity of properties.

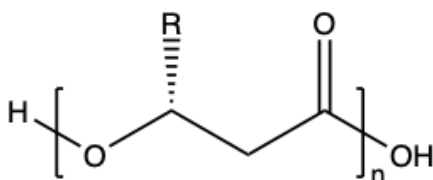


**Figure 2.** General structure of PHA monomer

PHA are distinguished by excellent thermoplastic and elastic properties, especially those of the MCL type, making them analogous to plastics derived from fossil sources. This similarity allows for a wide range of applications. The composition of PHA can vary depending on the organic substrate supplied to the microorganisms during culture. For example, the use of carbohydrates, lipids, or organic acids as carbon sources in nutrient-deficient cultures (e.g., phosphate, nitrogen, or dissolved oxygen) affects the length of monomeric units in the polymers, resulting in different properties (Khanna and Srivastava, 2005). Currently, at the industrial level, PHA production is mainly based on substrates such as glycerol, simple sugars and vegetable oils. However, processing these refined materials involves high costs, posing a significant obstacle to their competitiveness with conventional plastics, whose cost is significantly lower. Actual production costs of PHA are around €5-6/kg, while commonly available petrochemical plastics are around €1/kg (Jaquel et al. 2008). The predominant share of production costs is associated with raw materials, accounting for 50 percent of the total (Shen et al. 2009). Due to the cost challenge, research is moving toward the use of low-impact feedstocks, such as organic wastes or even gaseous substrates such as CO<sub>2</sub>. The use of waste materials is a promising option, as it could reduce costs and the environmental impact associated with PHA production and, concomitantly, mitigate gas emissions. Despite current economic limitations, the use of such polymers as substitutes for traditional plastics enjoys great interest both for the industrial sector and for the sake of the environment.

## 1.2. Poly(3-hydroxybutyrate): Properties, Challenges, and Potential

Among the various types of PHA, the best known is polyhydroxybutyrate (PHB), first isolated by M. Lemoigne from *Bacillus megaterium* in 1926. PHB is one of the most promising biopolymers gaining considerable attention, which falls into the category of SCL PHA. It is a linear polyester consisting of 3-hydroxybutyric acid, characterised by high crystallinity and brittleness (Preustig et al., 1990). It is



produced through bacterial fermentation processes by a wide range of both Gram-negative and Gram-positive bacteria. PHB granules are synthesised and stored as C and energy reserves under conditions of nutritional deficiency, and because of their complex structure are sometimes referred to as "carbonosomes." Their composition is predominantly PHA at 97%, followed by PHA-associated proteins 2% and lipids 1% (Jendrossek, 2009). These granules accumulate in the cytoplasm, exhibiting diameters ranging from 0.2 to 0.5  $\mu\text{m}$  (Khanna and Srivastava, 2005).

PHB's chemical and physical properties make it similar to plastics derived from fossil fuels, such as polypropylene (PP) and polyethylene (PE). Its high crystallinity gives it excellent mechanical properties (Yeo et al., 2017), while its lamellar structure promotes its resistance to gas permeability, making it suitable for applications in packaging and wrapping (Koller et al., 2010). One notable aspect is its biodegradability and biocompatibility, as the degradation product of PHB, D-3-hydroxybutyrate, is a common intermediate metabolite in many organisms, including humans, paving the way for potential biomedical applications (Holmes, 1985). The ecological properties of PHB place it as an alternative to conventional plastics, as it can be degraded in both aerobic and anaerobic environments without releasing toxic substances (Tokiwa et al., 2009). However, despite its interesting properties, PHB is plagued by some inherent limitations. For example, its slow crystallisation rate at temperatures below 60°C or above 130°C can promote the formation of spherulitic aggregates, imparting greater brittleness to the material (Ding and Liu, 2013). In addition, the melting temperature (200°C) is close to the degradation temperature, limiting opportunities for thermal processing (Yeo et al., 2017). High production costs are another significant obstacle. To overcome these limitations, various approaches have been developed, including mixing PHB with other materials (Bugnicourt et al., 2014). In addition, studies have been conducted to improve the physical properties of PHB, such as the production of copolymers such as polyhydroxybutyrate-co-hydroxyvalerate (PHBV). This copolymer can also be obtained through modifications to the C-based raw materials of the culture medium used in microbial biosynthesis.

From this perspective, the use of alternative inexpensive C sources, such as CO<sub>2</sub> or volatile fatty acids (VFA), emerges as a promising strategy to fuel microbial growth and copolymer synthesis. VFA, for example, are by-products generated during the anaerobic digestion (AD) of organic waste. Taking advantage of this dual resource, without the need for complex separation of VFA from digestates, can greatly lower production costs. In addition, the presence of a variety of volatile acids in digestate can enrich the production of copolymers with specific characteristics (Jawed et al., 2022). Different microorganisms that are able to use sustainable resources and waste materials as substrates have been studied for PHB production, among them, *Cupriavidus necator*, *Bacillus megaterium*, *Bacillus safensis*, *Pseudomonas oleovorans* (Brandl et al., 1990; Sirohi et al., 2020).

The use and the available knowledge of *C. necator* as a PHB producer makes it an optimal microorganism given its versatility in using waste substrates as C sources (Vu et al., 2022). This characteristic positions *C. necator* as an optimal candidate for transforming waste gases and materials into valuable biopolymers.

### 1.3. *Cupriavidus necator* as a versatile organism for PHB production

*C. necator*, initially known as *Ralstonia eutropha*, emerges as a model organism in the field of PHB production, exploiting a wide range of C sources. Belonging to the *Burkholderiaceae* family and classified as a Gram-negative bacterium, *C. necator* is distinguished by its extremely versatile metabolism. This characteristic allows it to function both as a heterotroph, using reduced organic compounds as electron donors, and as a chemolithotroph, employing gaseous H<sub>2</sub> as an electron donor. The bacterium uses oxygen (O<sub>2</sub>) as a final electron acceptor in aerobic growth, but is also able to grow anaerobically using nitrate as a final acceptor (Pohlmann et al., 2000). In the heterotrophic case, *C. necator* also uses the reduced C substrates, while in the chemolithotrophic case it draws C from CO<sub>2</sub>. This is made possible by the expression of ribulose-1,5-bisphosphate carboxylase/oxygenase (RuBisCO) and the subsequent fixation of CO<sub>2</sub> through the Calvin-Benson-Bassham cycle (CBB). One metabolic

aspect of considerable interest concerns the two *C.necator* hydrogenases involved in hydrogen (H<sub>2</sub>) oxidation. One is membrane-bound (MBH), involved in the electron transport chain, while the other, located in the cytosol (SH), is responsible for generating the reducing potential (NADPH) (Bowien and Schlegel, 1981). Both of these hydrogenases belong to the Ni-Fe class and have a bimetallic catalytic core located deeply within the larger subunit of a heterodimeric protein. It should be emphasised that the formation of this multi-active site occurs through several tightly regulated steps. Currently, the transcriptional factors involved in regulating the expression of the various subunits and the maturation process of both hydrogenases are being carefully analysed, with the goal of maximising the efficiency of CO<sub>2</sub> fixation. (Kim et al., 2022).

#### 1.4. Metabolic overview

With regard to heterotrophic growth, *C. necator* can use various substrates, including sugars such as fructose, N-acetyl-glucosamine, glycerol and even VFA. An exhaustive list of substrates potentially usable by the wild-type strain of *C. necator* (H16) has been formulated before (Pearcy et al., 2022). As for fructose, this carbohydrate is captured by the cell and initiates its metabolic pathway through the Entner-Doudoroff (ED) pathway, where it is converted to glucose-6-phosphate. Pyruvate derived from sugar degradation is subsequently oxidised to acetyl-CoA and feeds the tricarboxylic acid cycle (TCA), culminating in the production of CO<sub>2</sub> as the end product of the cellular respiration process. The reduced cofactors generated by such metabolic pathways play a crucial role in oxidative phosphorylation, with O<sub>2</sub> acting as the final acceptor (**Fig. 3**).

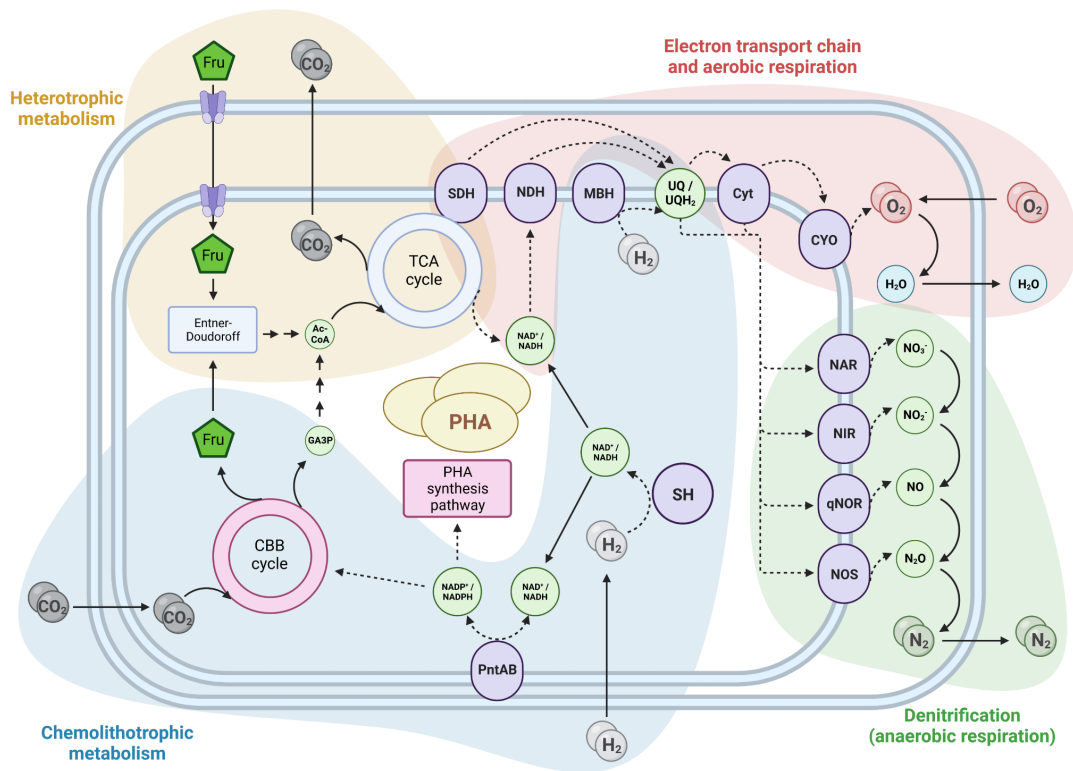


**Figure 3.** Metabolic overview of *C. necator* electron flows are represented with dotted arrows, metabolite/carbon flows with solid arrows. Violet elements are oxidoreductases, light blue are catabolic pathways, red are anabolic pathways. Abbreviations and gene symbols used in this figure: Fru, fructose; Ac-CoA, acetyl-coenzyme A; TCA, tricarboxylic acid; SDH, succinate dehydrogenase; SH, soluble hydrogenase; MBH, membrane-bound hydrogenase; PntAB, transhydrogenase; CBB, Calvin-Benson-Bassham; GA3P, glyceraldehyde-3-phosphate; NDH, NADH dehydrogenase; UQ, ubiquinone, Cyt, b/c-type cytochrome; CYO, cytochrome oxidase; NAR, nitrate reductase; NIR, nitrite reductase; NOR, nitric oxide reductase; NOS, nitrous oxide reductase. Created with BioRender.com.

It should be noted that *C. necator* is unable to express the enzyme 6-phosphogluconate dehydrogenase, which plays a key role in the pentose phosphate pathway (PPP) and plays an important NADP<sup>+</sup> supply function in most prokaryotes (Spaans et al., 2015). Therefore, the balance between NADP<sup>+</sup> and NADPH within the cell is maintained through the activity of the enzyme isocitrate dehydrogenase within the TCA (Fig. 3). It is likely that in *C. necator*, the pool of NADH and NADPH is regulated mainly by the presence of the membrane-associated transhydrogenase

enzyme PntAB, which catalyses the transfer of hydride ions from NADH to NADP<sup>+</sup> (Raberg et al., 2011; Sauer et al., 2004). However, interestingly, no evidence of NAD<sup>+</sup> reduction has been reported despite reversible transhydrogenase activity.

Regarding glucose, it is important to note that one of the most studied strains of *C. necator*, the H16, lacks the ability to utilise it, likely due to the absence of specific transporters (Raberg et al., 2011). Over the years, mutants have been isolated that, in contrast, are able to grow using glucose as a C source (Konig et al., 1969; Raberg et al., 2011).

### 1.5. Poly(3-hydroxybutyrate) production in *C.necator*

As commented above, *C. necator* proves to be a promising candidate for PHB production from CO<sub>2</sub>, with the ability to accumulate granules that can account for up to 65% of the cell's dry weight (Lu and Yu, 2017). Usually, batch reactors in which a mixture of H<sub>2</sub>, O<sub>2</sub> and CO<sub>2</sub> is introduced are used for PHB production from gas streams. The use of *C.necator* under autotrophic conditions has resulted in a significant reduction in raw material costs for PHB production. The CO<sub>2</sub> derived PHB production has already been demonstrated, and several approaches have been investigated to ensure optimal consumption, efficient growth, and consequent yield (Mozumder et al., 2014; Garcia-Gonzalez et al., 2015; Lu and Yu, 2017).

PHB synthesis in *C.necator* can be traced to three main enzymes: phaA, phaB and phaC. 3-ketothiolase (phaA) catalyses the condensation of two acetyl-CoA molecules, forming acetoacetyl-CoA. The latter is then reduced to 3-hydroxybutyryl-CoA through NADPH-dependent acetoacetyl-CoA reductase (phaB). Finally, PHA synthase (phaC) lengthens the PHB chain by adding 3-hydroxybutyryl-CoA. PHB accumulation in *C. necator* increases with the application of nutrient stress, increasing the C/N ratio in the medium. The choice of the limiting nutrient and the timing of its application have been shown to significantly influence polymer production (Choi and Lee, 1997).

A significant limitation has been identified in the dissolution of gases (CO<sub>2</sub>, O<sub>2</sub> and H<sub>2</sub>) in the liquid phase, a characteristic that is highly dependent on temperature,

pressure and agitation system. Optimal growth conditions for mesophilic bacteria such as *C.necator* are between 30°C and 37°C (Sheu et al., 2012). However, the limited solubility of the gases introduced to the growing culture at that temperature, has prompted ongoing efforts to overcome this issue, such as increasing the fermentation pressure or testing different reactor configurations to increase the gas-liquid transfer rate (Yu and Munasinghe, 2018). Since O<sub>2</sub> is one of the main limiting factors in growth, a specific H<sub>2</sub>:O<sub>2</sub>:CO<sub>2</sub> gas ratio of 7:2:1 had to be adopted to achieve adequate growth and prevent possible gas-related restrictions (Takeshita et al., 1996). However, this ratio carries the risk of falling within the explosive hazard range due to the presence of H<sub>2</sub> and O<sub>2</sub> in the mixture. Consequently, several options for an alternative feeding approach have been explored. Among the alternatives considered to overcome this issue there is the use of different electron acceptors from O<sub>2</sub>, such as nitrate. However, this option has been shown to significantly reduce cell growth (Tiemeyer et al., 2007). Another strategy contemplated has been to reduce the O<sub>2</sub> content below the explosive level. It is important to note that the lower explosive limit (LEL) for the mixture of O<sub>2</sub> and H<sub>2</sub> has been estimated to be between 4% and 6.9% by volume, respectively (Ishizaki et al., 1993; Schröder et al., 2007). However, a reduction in O<sub>2</sub> concentration below the LEL results in an increased risk of limiting the mass transfer.

The use of VFA in *C. necator* has been used for PHB production given their economy and the possibility of producing copolymers (Jawed et al., 2022), as mentioned above. However, limitations related to the pH of the medium and the concentration of some VFA can affect growth (Kedia et al., 2014).

#### 1.4. Aim of the thesis

The present study aims to investigate the biomass and PHB accumulation in *C. necator* using different C sources, studying both, heterotrophic and autotrophic metabolisms. The rate of gas consumption and production involved in the growth of *C. necator* was investigated, as well as crucial aspects related to the maintenance of cultures under autotrophic conditions and the conversion of substrates into PHB

polymers. The main objective is to examine the effect of physiological stress induced by nutrient deficiency, such as nitrogen and phosphorus, as a strategy to enhance PHB production through simultaneous carbon dioxide assimilation.

In the course of the research, several experimental conditions were investigated, including transition of C source from glucose to carbon dioxide utilisation, nutrient deprivation, and growth in the presence of volatile fatty acids. These conditions were designed to stimulate physiological responses in *C. necator* and promote PHB accumulation.

A key element involves the use of transcriptomic analysis, which aims to understand the molecular mechanisms and the crucial genes involved in the transition from heterotrophic growth on glucose to chemolithotrophic growth on carbon dioxide. This process includes the analysis of gene expression during the adaptation period in order to provide insights into the metabolic pathways that regulate *C. necator* growth under the different experimental conditions and lead to PHB production.

The results obtained from this study have relevant implications in terms of environmental sustainability and biopolymer production. They contribute to the understanding of the dynamics related to the removal of greenhouse gases during the microbial growth process and the simultaneous production of high-value products such as PHB from waste streams. This cutting-edge approach contributes to greater integration of sustainable production, biotechnology research and environmental impact reduction, paving the way for better resource management and innovative solutions in the area of environmentally friendly materials production in a circular economy frame.

## 2. Materials and Methods

### 2.1. Bacterial strain and inoculum preparation

The DSM 545 strain of *C. necator* used in this thesis project was supplied by the Leibniz Institute DSMZ collection (Braunschweig, Germany). The strain is a mutant derived from strain H1 (DSM 529) capable of using glucose as a growth substrate, which is linked to constitutive expression of the gene for glucose-6-phosphate dehydrogenase. *C. necator* DSM 545 was maintained at -80°C in a 25% glycerol solution and activated, when needed, at ambient temperature in Nutrient Agar medium peptone 5 g/L, yeast extract 2 g/L, NaCl 5g/L, meat extract 1g/L, and agar 13 g/L. For the set-up of the experiments, the strain was grown in Petri dishes using nutrient broth medium (NB) and agar (1% w/v). Biomass from the Petri dish was used for the inocula in an Erlenmeyer flask, which were grown using Medium 81 (Deutsche Sammlung Mikroorganismen DSMZ, <http://www.dsmz.de/>, Germany) supplemented with glucose (5 g/L), incubated at 30°C on orbital shaker (200 RPM) for 48 hours.

### 2.2. Culture set-up and media preparation

Medium 81 was prepared following instruction of DSMZ (<http://www.dsmz.de/>, Germany), starting from MilliQ water (1L) autoclaved at a temperature of 121°C to ensure complete sterilisation of the culture medium. Once the water was cooled, 10 mL (10 mL/L) of previously autoclaved solution A, B and C were added under a laminar flow hood. Finally, 0.5 mL (0.5 mL/L) of standard vitamin and trace element solution was added, the components of the medium are listed in **Appendix (Section A)**. The glucose was first dissolved in a given volume of MilliQ water and then filtered through a 0.2 um filter so as to ensure the sterility of the solution added to the medium. To this mixture, 0.5 mL of microelement solutions were added per 1 L of Medium 81. Additionally, the standard vitamin solution was supplemented.



### 2.3. CO<sub>2</sub> adaptation of maintenance culture

Three batch experiments were performed to test the adaptation from glucose to CO<sub>2</sub> in terms of biomass accumulation. The first experiment was performed in 120 mL glass bottles with 40 mL of working volume and 80 mL of headspace. The experiment was conducted in two stages: initially cultivating *C. necator* aerobically in an Erlenmeyer flask with glucose (5 g/l), subsequently employing the inoculum culture as a 10% v/v for batch bottles. Each bottle was sealed tightly with butyl rubber stoppers sealed with aluminium clips. Sampling and gas additions were done using syringes with sterile needles to keep the gaseous composition of the headspace controlled. Specifically, maintenance operations included periodic addition of gas, taking samples for gas chromatography, and aliquots for optical density measurements. The bottles were initially fed with a mixture of H<sub>2</sub>:O<sub>2</sub>:CO<sub>2</sub> in the proportions of 5:1:1. The experiment lasted 14 days, with 120 mL of gas injected daily during the first 7 days (varying volume of H<sub>2</sub>:O<sub>2</sub>:CO<sub>2</sub> depending on the gas chromatography). During the next 7 days, 60 mL was added. As O<sub>2</sub> was rapidly consumed, 70 mL more than the initial 20 mL was introduced.

A second experiment was performed following the same procedures, consisting in scaling-up the processing of 550 mL glass bottles in order to evaluate the adaptation of the microorganism on larger volumes. The working volume was 180 mL, with 171 mL of glucose-free medium 81 and 9 mL of inoculum obtained by mixing the triplicates from the previous experiment. The amount of gases introduced was increased correspondingly, respecting the following proportions: 200 mL of H<sub>2</sub>, 100 mL of CO<sub>2</sub> and 70 mL of O<sub>2</sub>. From day 7 the gas amounts were kept constant in all replications to closely monitor consumption and production rates. At this stage of the adaptation, no samples were taken for analysis of PHA produced. The experiment was concluded by combining the remaining bottles to use the volume as inoculum in the subsequent adaptation step.

In the final step (third experiment), the volume was maintained and bottles were prepared from the previous experiment, with an additional control adding glucose (5

g/L). In the three autotrophic replicates refilling of gases was performed with constant volumes of gases each day, and in all bottles the growth was monitored.

## 2.4. Analytical methods

Liquid and gas samples were taken regularly to control biomass accumulation and gas production or consumption. Biomass growth was quantified by assessing the optical density (OD) measuring the absorbance at 600 nm (OD<sub>600</sub>) using a Spark® multimode microplate reader (Tecan, Switzerland). OD readings were taken using a Costar (Corning) 96-well transparent plate, in triplicate. Gas analyses were conducted using a gas chromatograph (Agilent 8890 Series Gas Chromatograph), using N<sub>2</sub> as inert carrier gas and a thermal conductivity detector (TCD). Analyses of headspace composition were performed by inserting 1 mL of gas into the injection chamber of the chromatograph. Peak integration, calibration, and data processing were performed through OpenLAB Chromatography Data System (CDS) software. For analysis of VFA, the same gas chromatograph was used, but analyses were performed using a flame ionisation detector (FID), using helium as carrier gas. VFA samples were prepared according to the following protocol: 1 mL was taken to which 40 µL of orthophosphoric acid (40 µL/mL sample) were added; the sample was centrifuged at 15000 RPM for 10 minutes at room temperature; finally, the supernatant (1 mL) was transferred to a vial specific for gas chromatograph analysis with the addition of 100 µL of 4-methyl valeric acid (which served as an internal standard).

## 2.5. Alternative carbon sources experiment set-up

In the preparation of cultures in the presence of VFA, medium 81 was used with additions of specific volumes of glacial acetate solutions, synthetic mixtures of VFA, and digestate from an industrial biogas plant. The pH was corrected to an appropriate growth value of about 6.5, using a 1M NaOH solution. The added volumes of VFA or digestate were calculated to obtain a C molarity comparable to that present in a 5 g/L solution of glucose. The C content in glacial acetate was determined by calculating that of an acetic acid molecule (CH<sub>3</sub>COOH) and converting it to molarity. The

amount of C in one gram of acetic acid was calculated as 0.399 g C/g CH<sub>3</sub>COOH. The molarity of C in solution was found by using the molarity of acetic acid (17.416 mol/L) and was determined as 6.96 molC/L. To achieve a final concentration of 50 mM C, the dilution equation  $C_1V_1 = C_2V_2$  was used. Starting with a 6.96 mol/L glacial acetate solution of 40 mL, the volume needed for the new concentration (0.05 mol/L) was calculated as 222.72 mL. Thus, 0.287 mL of glacial acetate solution was used for a final solution of 50 mM C concentration. The C moles per litre for each acid in the mixture were determined for the volume of the mixture of VFA (0.76 mL) composed as in **Table B1** in **Appendix (Section B)**.

Instead, the volume of digestate (1.28 mL) was calculated based on its acetic acid content measured with a gas chromatograph (see paragraph 2.4). The digestate was previously filtered and centrifuged. Subsequently, an experiment was conducted in which the responses of the microorganism to different concentrations of acetate (0.6 g/L - 1.2 g/L - 3.0 g/L) were evaluated. Cultures were prepared in 120 mL bottles with a working volume of 40 mL. Initially, 35 mL of medium 81 was added, after which acetate was added at the desired concentration and the pH was adjusted using 1M NaOH: 300 uL in the first condition, 600 uL in the second and 1.7 mL in the third. Finally, 2 mL of inoculum was added to start the culture.

Two experiments were performed to test the growth of *C. necator* on VFA. The experiments were performed in 120 mL glass bottles, with 80 mL headspace and 40 mL working volume (36 mL glucose-free medium 81 and 4 mL inoculum). As explained in paragraph 2.1, a previous step for growing with glucose was performed. In the first experiment, twelve bottles were prepared: two controls with only medium 81 and two with glucose (5g/L), triplicates with a mixture of VFA, three with digestate that originated from a biogas plant processing agroindustrial residues, and three with acetate. In the second experiment, different concentrations of acetate were tested in duplicates: 0.6 g/L - 1.2 g/L - 3.0 g/L, in 120mL bottles. The experiment continued for two weeks, with daily measurements of OD and VFA sampling every few days.

## 2.6. Nitrogen and phosphorus starvation media

To induce nutritional stresses, media without nitrogen (N) or phosphorus (P) compounds were prepared. For the preparation of the first, ammonium chloride-free storage solution B was made as specified in **Appendix A**; in the second case, storage solution C containing ferric ammonium citrate was not added during the medium preparation. The pH was determined using litmus paper (MQuant Merck KGaA) and set to a value of 6.9.

### 2.6.1. Heterotrophic N and P starvation

The inoculum preparation was set to 24 hours (see paragraph **2.1**). 5% of the inoculum flask sample was transferred into four 50 mL Falcon tubes. The tubes were centrifuged for 2 min at 3000 RPM at room temperature, and the resulting pellet was resuspended in a medium 81 volume appropriate to obtain a final OD value of 0.2. The two conditions were set up under N and P deficiency by preparing the medium as explained before. In this specific case, organic C (5 g/L glucose) was used. The starvation lasted for 48 hours, and subsequently, the observation and quantification of PHB granules were carried out using Nile-Red staining daily (see paragraph **2.6.3**).

### 2.6.2. Autotrophic N starvation

The experimental protocol involved an initial phase in which there was the adaptation to the autotrophic condition, employing CO<sub>2</sub> as the C source. Two replicate setups of 550 mL each were prepared, following the same procedure described before (see paragraph **2.3**). Eight bottles were prepared: four containing medium 81 and the other four containing modified medium 81 (see paragraph **2.5**). The starvation period persisted for seven days. Throughout both the adaptation and starvation phases, samples were collected daily for OD measurements (see paragraph **2.4**), while at the end samples for PHB extraction were collected (see paragraph **2.8**).

In this experiment two different atmospheric pressure conditions, crucial factor influencing the growth of *C. necator*, were tested following suggestions from DSMZ. Previous studies, conducted by Yu and Munasinghe (2018), showed that pressure

values between 1 and 4 atm led to higher cell density produced by the culture. Based on this, it was decided to make changes in the volumes of gases used, but keep the pressure levels exerted by the gases inside the bottles constant at 2 atm. As a result, the gas volumes under the respective conditions were differentiated; on one side a normal atmosphere condition (10% O<sub>2</sub>, 40% N<sub>2</sub>, 8% CO<sub>2</sub>, 41% H<sub>2</sub>) was ensured, while in the remaining replications a modified condition (10% O<sub>2</sub>, 71% N<sub>2</sub>, 8% CO<sub>2</sub>, 10% H<sub>2</sub>) was applied. This last atmosphere has been suggested for N starvation from DSMZ, but no experiments comparing the two atmospheres has been found in literature. Daily gas refilling was performed according to the set condition to keep the relative percentages of gases constant in each bottle, the remaining internal pressure was released before refilling.

### 2.6.3. Nile-Red staining

For observation and quantification of PHB granules, Nile-Red dye was used. Two Eppendorf tubes were prepared for each condition, one stained with a final concentration of 1.25 µl/ml Nile-Red, and the other not stained as negative control. An additional tube with water stained with Nile-Red was used as control. The samples were then incubated at 37°C for 30 min in the dark to allow complete staining. Finally, fluorescence was measured using a Tecan system and a 96-well Nunc (Thermo Scientific) black plate, in triplicate. Excitation and emission wavelengths used were 485 and 580 nm, respectively. The data obtained were then analysed and corrected for the contribution of the Nile-Red signal in water and for the contribution of cells alone. The Leica SP5 confocal microscope was used and observation of PHB granules was done *in vivo*. Slides were prepared with 2 µL of sample, and visualised by using the HCX PL APO lambda blue 63.0x1.40 OIL UV objective. Nile-Red was observed by exciting samples at 488 nm with an Argon laser and by detecting it at 500-590 nm.

## 2.7. Transcriptomic experiment

### 2.7.1. Culture preparation and maintenance

RNA sequence analysis was performed on two different cultures under adaptation. Twelve 550 mL bottles with a working volume of 180 mL each were set up. In eight of these bottles, 162 mL of medium 81 (4 containing 5 g/L glucose and 4 without glucose) was added, followed by 18 mL of inoculum (10% of the total working volume) from an Erlenmeyer flask grown for 24 hours at 30°C. The remaining four bottles were prepared by adding 171 mL of glucose-free medium 81 and 9 mL of inoculum (5% of the total working volume) taken from the bottles of the previous adaptation experiment. Four controls were then obtained, four bottles with 10% inoculum from the flask and four bottles with 5% inoculum from the previous experiment. In the eight bottles without glucose, 250 mL of H<sub>2</sub>, 50 mL of CO<sub>2</sub> and 70 mL of O<sub>2</sub> were added, yielding an initial pressure of about 2 atm. The same amounts of gases were added daily and the internal pressure of each bottle was measured using a pressure gauge. The gas percentages were measured by the gas chromatograph. In bottles without glucose, every 24 hours, overpressure was released through a needle placed on the bottle cap. Subsequently, gases were refilled and pressure and gas composition were measured again.

Pressure and gas percentage values were used to calculate the equivalent volume of each gas at 1 atm. The calculation was performed using the perfect gas state equation to obtain the moles for each gas species:

Utilising the ideal gas law  $PV = nRT$ , it was determined the moles of each gas species considering that, at 1 atmosphere, 1 mole occupies 22400 mL (at 0°C). By applying the measured pressure, we calculated moles (n). In this equation, P stands for measured pressure, V for headspace volume (0.32 mL), R for universal gas constant (0.082057 L atm K<sup>-1</sup> mol<sup>-1</sup>), and T for temperature in Kelvin (303 K).

### 2.7.2. RNA extraction and sequencing

For RNA extraction, 15 mL of culture were centrifuged at 4000 g for 10 minutes at 4°C. Total RNA was extracted from the resulting pellets using TRIzol™ reagent (Thermo Fisher Scientific, USA) following the manufacturer's instructions. After resuspension of the sample, 200 uL of chloroform was added and the tubes were incubated at room temperature for 3 min and centrifuged at 4°C for 15 min at 12000 RPM. The aqueous phase was transferred into clean 1.5 mL eppendorfs, adding 500 uL of isopropanol and incubating for 10 min at room temperature. After centrifugation at 4°C for 10 min at 12000 RPM, the supernatant was discarded and the pellet was washed in 1 mL of 80% ethanol, centrifuged again at 4°C for 5 min at 7500 RPM, discarding the supernatant and drying the pellet. Finally, the pellet was incubated at 55-60°C for 10-15 min. RNA samples were quantified through Qubit and Nanodrop and stored at -80°C. To eliminate DNA contamination, the extracted RNA was treated with DNase I provided with the RNA Clean & Concentrator™ kit (Zymo Research, USA). The QIAseq FastSelect kit (Qiagen, USA) was used to mask ribosomal RNAs. Libraries were prepared using the Illumina Stranded mRNA Prep (Illumina Inc., San Diego CA), and the sequencing was performed on the Illumina Novaseq 6000 platform (2 × 150, paired end) at the sequencing facility of the Department of Biology, University of Padua.

### 2.8. PHA extraction and analysis

For the analysis of PHA produced by the cultures, it was necessary to calculate the dry weight of the starting cell material. Samples were first placed in weighted 50 mL Falcon tubes and then centrifuged for 30 min at 4000 RPM at 4°C. After centrifugation, pellets were separated from the supernatant and stored at -20°C until they were lyophilized. To avoid the weight of tubes from being altered by the presence of moisture the empty tubes were subjected to a drying process prior to collection, which consisted of a first step in a desiccator for 12 hours and a second step in a vacuum bell for one hour. After the drying procedure was completed and the tares were weighed, the volumes of samples to be processed were placed inside the

tubes. For the preparation of PHA samples for analysis, the protocol of G. Braunegg et al. (1978) was followed, which includes a specific procedure for extraction and purification of the polymer. Each sample was placed in a -80°C freezer for 24 hours. Subsequently, the frozen samples were transferred to an Edwards lyophilizer at -60°C for an additional 24 hours. The resulting samples were then weighed. For PHA extraction, 10 mg of lyophilized pellet were dissolved in a mixture of 2 mL of acidified methanol and 1 mL of chloroform within a PYREX screw-cap tube. The tube was then incubated at 100°C for 60 minutes. After cooling to room temperature, 1 mL of distilled water was added to the mixture, and the sample was shaken for 10 minutes to facilitate phase separation. The resulting organic phase was then collected for analysis using a gas chromatograph.

## 2.9. Gene expression analyses

To perform the transcriptomic analysis, the genome sequence for *C. necator* H16 (RefSeq ID: GCF\_000009285.2) was employed, considering its annotation and the good alignment rate obtained. Raw reads were trimmed using Trimmomatic v0.39 with the options "-phred33 LEADING:20 TRAILING:20 SLIDINGWINDOW:4:20 MINLEN:70" and clipped with BBDuk v38.86 to remove adapters. The trimmed and filtered reads were then aligned to the reference genome using Bowtie2 v2.5.1. Read count tables were generated by extracting the number of reads mapped within each gene with HT-Seq v2.0.2 (Anders et al., 2015), using options "--nonunique=fraction -m intersection-nonempty -s no -a 0". Differential expression (DE) analysis was conducted using DESeq2 (v. 3.14) (Love et al., 2014), comparing CO<sub>2</sub>-adapted and non-adapted cultures against glucose. The results were filtered with an absolute log fold change (LFC) threshold set at 1. Benjamini-Hochberg correction for p-values was applied to each gene, and the threshold for the adjusted p-value (Q-value) was set at 0.05. Lists of significant differentially expressed genes were generated for each comparison. Principal component analysis (PCA) was performed using the 500 most variant genes as implemented by DESeq2. Gene annotations for *C. necator* H16 were obtained from the Kyoto Encyclopedia of Genes and Genomes (KEGG) database.



### 3. Results and discussion

A series of experiments were conducted to evaluate different growth strategies in order to optimise the performance of *C. necator*. These experiments were designed to explore the adaptability of *C. necator* to a variety of environmental conditions and carbon sources in order to identify optimal conditions for its use in PHB applications. The main conditions examined were growth using CO<sub>2</sub> as a carbon source, the use of VFA as a substrate, and growth in the absence of key nutrients, in order to explore the potential for PHB accumulation in situations of nutritional stress.

#### 3.1. Adaptation from heterotrophic to chemolithotrophic metabolism

Initially, the cultures needed an adaptation phase from a medium with glucose to a medium lacking any organic carbon source, but being fed with CO<sub>2</sub>. To do this, three adaptation steps were set up, and during each of them, the biomass growth and rate of consumption and production of gases were monitored. In the first phase, the addition of gases was not constant for each replicate, as it was chosen to add gases only when their concentration in the headspace, monitored by gas chromatography analysis, was close to zero. *C. necator* showed an increase in OD in all three replicates during the entire period of adaptation from glucose to CO<sub>2</sub> due to biomass growth (**Fig. 4a**). This is in accordance with Yu and Munasinghe (2018) study, in which the growth curve followed a linear trend. However, contrary to the results of Yu and Munasinghe (2018), the trend of the growth curve does not seem to reach a stationary phase (**Fig. 4**).

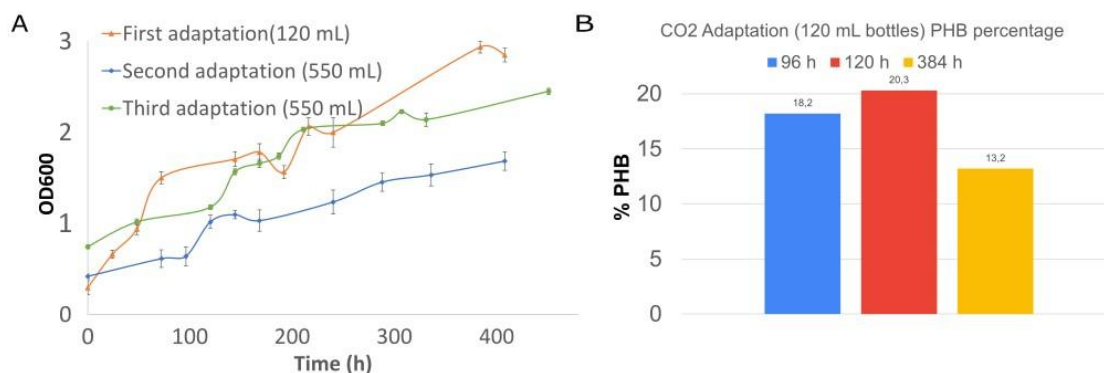


**Figure 4.** Autotrophic growth of *C.necator* during the three CO<sub>2</sub> adaptation steps, before and after scale-up. The graph depicts the growth trends as follows: the initial adaptation phase in 120 mL bottles is represented by the orange curve, the second adaptation phase after the scale-up to 550 mL bottles is shown in blue, and the third adaptation phase, also in 550 mL bottles, is represented by the green curve (a). PHB percentage during the first adaptation phase in 120 mL bottles (b).

Continuous growth can also be observed in the latter two phases, after the scale-up to 550 mL bottles (**Fig. 4a**). Overall, results show that growth is successful and maintained steadily over time, albeit at a very slow pace and following a linear trend. In contrast to what is observed in heterotrophic growth conditions (Mozumder et al., 2014), the autotrophic growth continues indefinitely within the limits of the adopted fermentation volume, without experiencing premature growth cessation due to glucose depletion. This phenomenon is attributed to the continuous addition of H<sub>2</sub>, O<sub>2</sub>, and CO<sub>2</sub> as energy and C sources allowing for continuous growth that would not be possible in a batch system with the presence of glucose alone. However, it is anticipated that this growth cannot extend infinitely without a renewal of the culture medium: over time, many nutrients will be depleted, contributing to the gradual decline in the growth rate. In conclusion, it can be stated that over the course of 400 hours, a clear stationary phase is not visibly evident.

During the adaptation period, 35 mL samples were collected for the analysis of the produced PHA. Despite not introducing specific conditions to stimulate PHB accumulation, a small percentage was observed on the total dry weight (**Fig. 4b**). This result indicates that a portion of the added CO<sub>2</sub> during the adaptation period was fixed and stored in the form of PHB granules. These findings suggest that by optimising the process and implementing conditions that induce accumulation, it is possible to enhance even more the PHB production. The study conducted by L. Garcia-Gonzalez et al. (2015) demonstrates that using fructose as the C source under heterotrophic conditions yields the best results for PHB production. However, it's worth noting that fructose and glucose can be expensive substrates, and in industrial settings, it is often more desirable to replace them with lower-cost or waste-derived substrates, like CO<sub>2</sub>.

It was possible to observe that a 20% accumulation rate was achieved after 120 hours, even in the absence of nutritional stress (**Fig. 4b**). This outcome underscores the important role of PHB granules as reserves during chemolithotrophic growth.

### 3.2. Exploration of carbon sources economically favourable

#### 3.2.1. Growth analysis on volatile fatty acids

The possibility of growing *C. necator* in media added with alternative C sources was tested. Specifically, the effect of using digestate, acetate or mixture of VFA was evaluated, comparing growth with a control in which the C source was glucose. In the first experiment conducted, three different sources of VFA were compared: digestate from an anaerobic digestion plant, mixture of pure VFA and glacial acetate. In all three cases, the growth of *C. necator* was lower than in the control with glucose (**Fig. 5a**). It is believed that the presence of acetate, digestate and mixture of VFA negatively affected the growth of *C. necator* probably due to the low pH observed in the medium (XYZ), which was less than 6.

In the 2022 study by Jawed et al. concentrations of individual VFA normalised to 50 mM C equivalent were used, with a specific concentration of 25 mM for acetic acid based on toxicity test results. In the current study, however, lower concentrations were employed (about 1 mM in the mixture of VFA and the digestate), which could have had a negative impact on growth performance, causing a prolonged adaptation phase. This phenomenon was also found in the case of high concentrations of acetic acid, where concentrations of 50 mM can cause a prolongation of the adaptation phase by up to 15 hours (Vu et al. 2022). In the experiment in which glacial acetic acid was used, the concentration adopted was 130 mM, higher than those previously reported in the literature. Although 1M NaOH solution was used in both experiments, in the second case this concentration was not sufficient to buffer the medium resulting in growth failure.

It is therefore more plausible that the acidity of the substrate exerted a great influence on growth. In particular, at pH levels below the pKa of individual VFA, the not dissociated form of these acids can easily penetrate the cell membrane, gaining access

to the cytosol, where their subsequent dissociation and subsequent acidification of the cellular environment takes place. This has the effect of reducing the proton gradient across the membrane, adversely affecting the rate of acid utilisation and hindering cell growth (Wang et al., 2010).

In particular, cell growth in the digestate-containing medium was slightly higher than in the conditions containing the mixture of VFA and acetate (**Fig. 5a**), but in all cases it was lower than in the glucose-containing control. However, it is important to consider that the medium in the presence of digestate turns out to be much more turbid than in the other media, due to the presence of organic matter that has not been completely filtered out.

In addition, to assess the utilisation of VFA for PHB production by *C. necator*, specific analyses were conducted on the individual VFA present in the culture media containing acetate, digestate, and VFA mixture. For this purpose, samples were taken along with those for OD and for gas chromatograph analysis to determine the consumption of VFA present in the cultures.

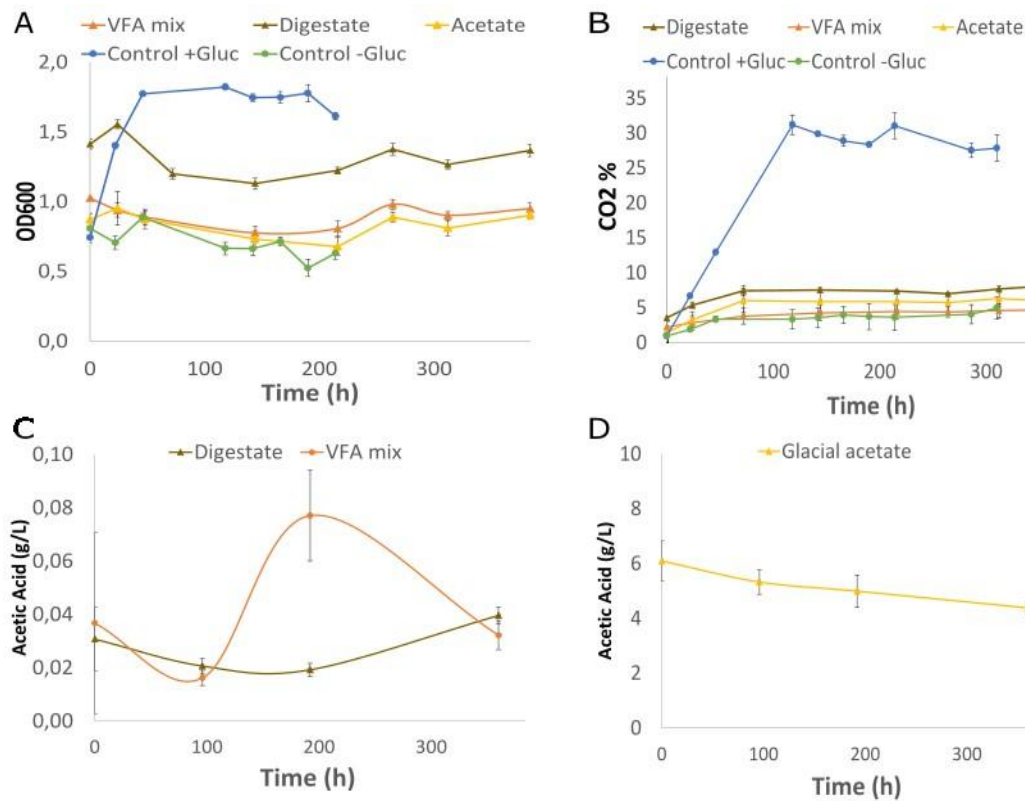


**Figure 5.** growth trend (a) and percentage of CO<sub>2</sub> (b) produced among different conditions; trends in consumption of acetic acid (g/L) present in cultures with digestate and mix of VFA (c) and glacial acetic acid (d), respectively.

When at appropriate levels VFA are metabolised into CO<sub>2</sub>, cell biomass and PHB (Yu et al. 2002). No significant increase in CO<sub>2</sub> levels was observed during growth (**Fig. 5b**). This may be attributed to the low utilisation of the VFA present, probably due to pH values as the utilisation of individual VFA was not evident, as can be inferred from the observed trends.

VFA could be effective C sources only if the pH and concentration are carefully controlled. In the context of the experiment, the low utilisation rate of these acids suggests an inhibitory effect, likely caused by excess acidity in the culture medium.

### 3.2.2. Growth analysis on acetic acid

A further experiment was carried out to evaluate the effect of varying acetate concentrations on cell growth and CO<sub>2</sub> production. Three conditions were tested: 0.6 g/L, 1.2 g/L, and 3.0 g/L acetate. It was previously shown that in batch cultures in media in which 5 g/L acetic acid was present, *C. necator* was able to deplete the entire C in the medium in the first 36 hours (Vu et al. 2022). It was noted in the previous paragraph that at these concentrations *C. necator* did not seem to be able to grow and consume the acetate present. However, in this specific experiment the different concentrations of acetic acid showed interesting behaviours of *C. necator* growth (**Fig. 6a**). Unfortunately, compared to the control with glucose, the culture did not reach high OD values. When adding 0.6 g/L of acetate, an initial lag phase was observed and *C. necator* was able to grow and consume the acetic acid present in the first 50 hours. This fact reflects the increase in the percentages of CO<sub>2</sub> present in the bottles, however, the OD slightly exceeds the value of 1, the maximum achieved before the beginning of the decreasing phase (**Fig. 6a**).

When 1.2 g/L of acetate were added, a faster growth rate than the other two conditions was observed, however, the rate of acetate consumption and consequently the rate of CO<sub>2</sub> production was not significantly affected. A slight growth was

observed but below the values reached in the previous condition, although growth at these concentrations was documented in the literature (Jawed et al., 2022). It is possible that, as in the previous experiment, the 1M NaOH concentration used as a buffer was not sufficient to balance the pH of the growth medium. In the last condition (3 g/L), no appreciable acetate consumption and consequent CO<sub>2</sub> production was shown, although *C. necator* growth can be seen.

It is possible to state that the preferable concentrations of acetic acid for *C. necator* are 0,6 g/L and 1,2 g/L, although in the latter case no appreciable consumption of the substrate was observed. The pH was monitored at the time when the culture was started, 6.5/7, and it was one of the most critical factors in growth. This aspect is crucial with regard to energy metabolism and should be monitored more closely in future experiments. A more concentrated base should also be used to prevent the introduction of excessive volumes to the medium for optimal *C. necator* growth. As no biomass growth was observed, no PHA production was also occurring.

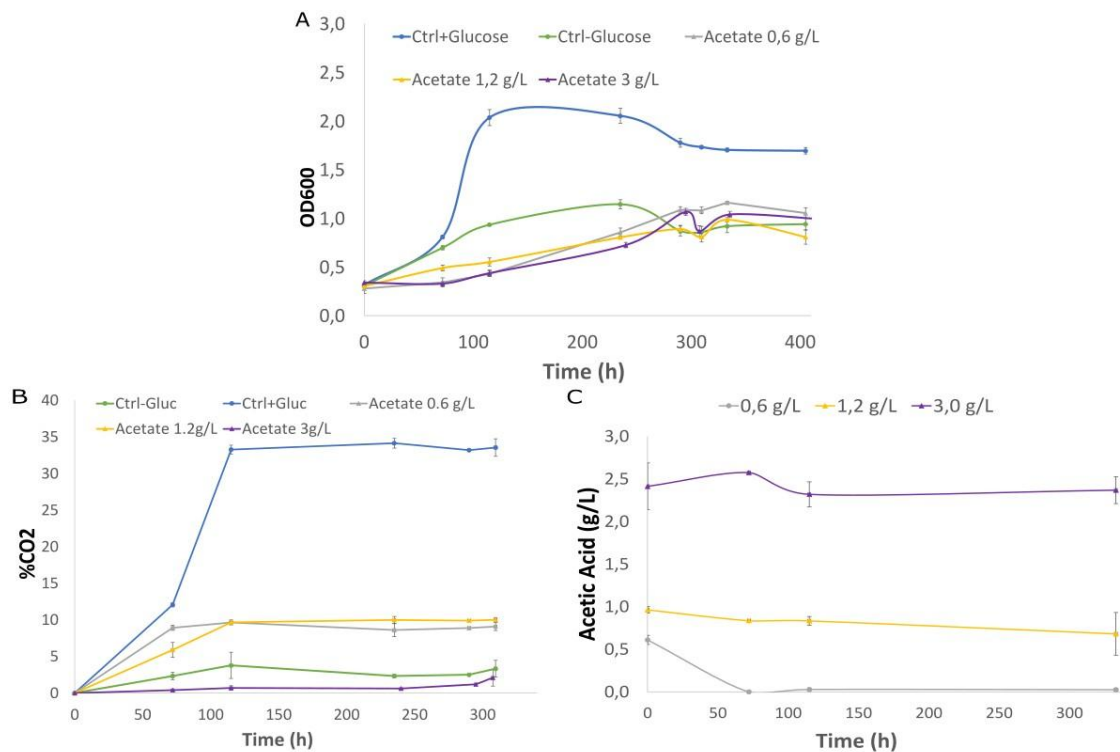


**Figure 6.** growth trend among media with and without glucose and different concentrations of acetic acid (g/L; a); CO<sub>2</sub> percentage production (b) and acetic acid consumption trend (c).

### 3.3. Nutrients starvation trials

#### 3.3.1. Heterotrophic growth trends during nitrogen and phosphorus starvation

Several studies have documented how the imposition of environmental stresses can induce the synthesis of PHB in *C. necator*. In particular, it has been shown that the deficiency of certain nutrients, such as N compounds, combined with an excess of C sources can lead to an increase in the accumulation of this polymer (Bellini et al., 2022; Horvat et al., 2013; Obruca et al., 2010). In the context of the following experiment, several cultures were initially grown under heterotrophic conditions, using glucose as the predominant C source and two different nutritional stress conditions were introduced, one characterised by H<sub>2</sub>PO<sub>4</sub> (P) deficiency and the other by NH<sub>4</sub>Cl (N) deficiency. Phosphate and ammonium limitations were previously documented in the study by Ryu et al. (1999), in which fed-batch cultures were conducted. In both cases, P and N concentrations were maintained at levels sufficient to ensure cell growth, and in both contexts, an increase in PHB accumulation rates was observed. In the current study, both stress conditions were performed in a situation of total absence of P and N (**Fig. 7**).

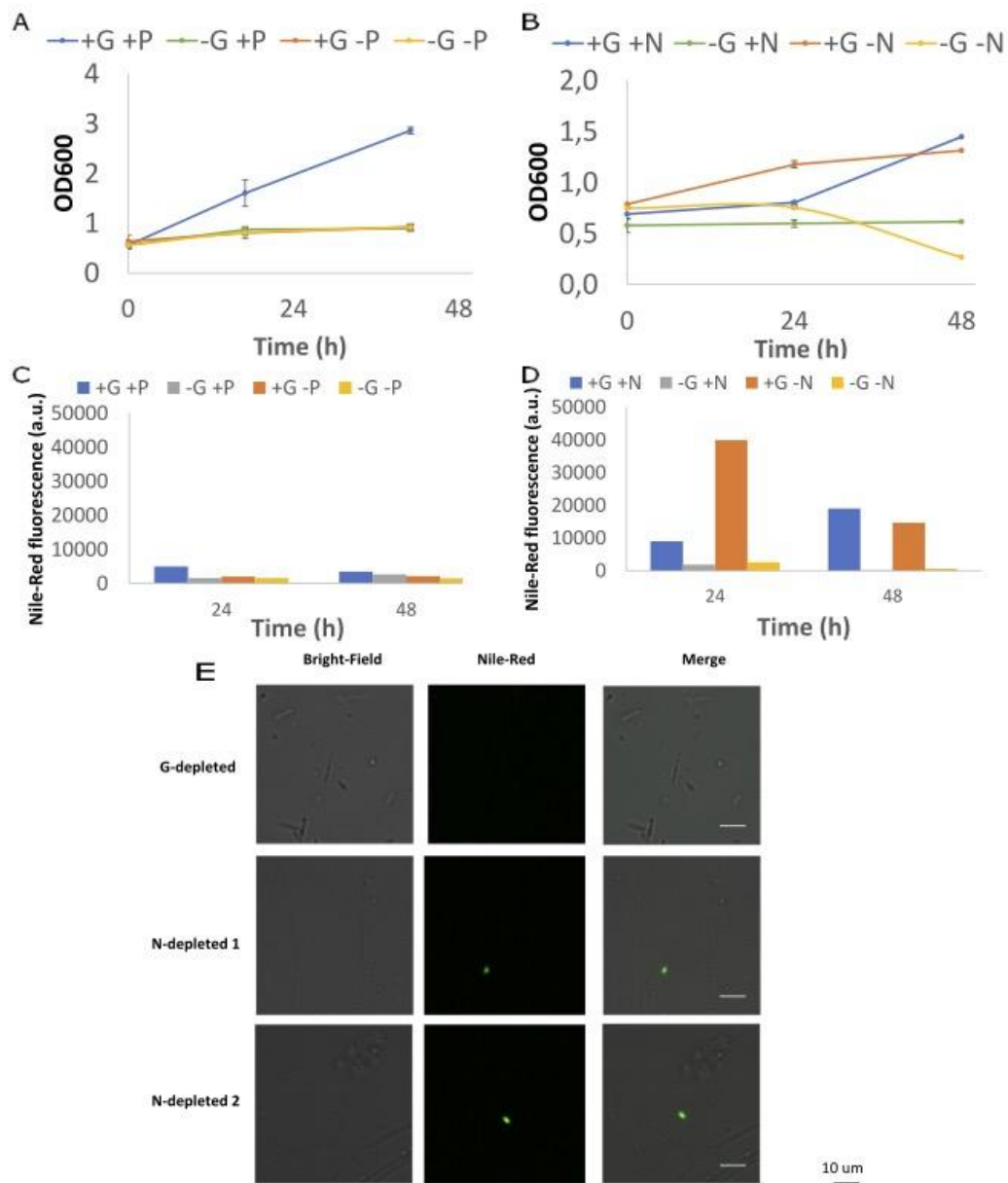


**Figure 7.** Growth trend in P (a) and N (b) starvation respectively. Nile-Red fluorescence among P (c) and N (d) starvation. Bright-Field, Nile-Red and merged images. *C. necator* is highlighted due to the presence of PHB granules stained with Nile-Red (e).

Growth profiles were monitored for the different conditions evaluated over 48 h. It can be stated that there was an obvious impact on the growth of *C. necator* due to phosphate deficiency (**Fig. 7a**). In this scenario, bacterial growth was only possible when both glucose and phosphate were present in the culture medium. Similarly, the



experiment involving N scarcity (**Fig. 7b**) shows that the presence of glucose is a prerequisite for any observable growth of the culture, given the absence of an alternative C source. It should be noted that minimal disparities were found when comparing growth patterns in the presence or absence of N.

Nile-Red dye was adopted as a means to reveal the presence of PHB granules under the different experimental conditions (**Fig. 7c,d**). In the context of phosphate deficiency the lack of this nutrient arrests growth, an effect that becomes even more evident through analysis with Nile-Red dye in phosphate-depleted cultures (**Fig. 7c**). This phenomenon is presumably attributable to the absence of growth, as the lack of sufficient biomass may prevent effective accumulation of PHB granules within the cells. The result is a poor response of Nile-Red, as evidenced by the presence of only one peak in the glucose- and phosphate-enriched culture, which, in contrast, manifested a normal growth process. The dynamics are different when it comes to N compound-free condition; a peak of fluorescence emerged at 24 hours, followed by a decrease at 48 hours. The impact of an excess of C sources in the absence of N compounds seems to lean toward an increase in the production and accumulation of PHB granules, especially in the early stages after N insufficiency (**Fig. 7d**). In addition, it was feasible to observe PHB granules within the cells of *C. necator* through staining with Nile-Red (**Fig. 7e**), as it serves as a lipophilic fluorescent probe capable of binding to lipid-like inclusions (Spiekermann et al., 1999).

### 3.3.2. Autotrophic growth trends during nitrogen starvation

In a subsequent experiment, N starvation was introduced under autotrophic conditions, using CO<sub>2</sub> as the C source and testing different pressures. In several studies, it has been found that pressure can play a significant role in the growth of *C. necator* under autotrophic conditions minimising the lag-phase. Specifically, in the study by Yu et al. (2018) it was shown that pressure values between 2 and 4 atm can increase cell growth. Similarly, partial gas pressure, such as O<sub>2</sub>, has been shown to

have an impact on growth under autotrophic conditions, as highlighted in the study conducted by Amer et al. (2023). Consistent with these findings, a change in gas composition was made between the two conditions: with and without N. Importantly, the total gas pressure in the headspace was kept constant by maintaining a gas ratio defined as "normal" and a gas ratio defined as "modified" (as described in the paragraph 2.6.2.). In the latter configuration, only N<sub>2</sub> and H<sub>2</sub> were changed in volume, while the total pressure was kept stable at 2 atm. Before introducing stress, a CO<sub>2</sub> adaptation step was performed, confirming the previous observation of steady, linear growth with continuous CO<sub>2</sub> consumption over the monitoring period (**Fig. C1 in Appendix Section C**).

Regarding growth in cultures with and without N in a normal atmosphere (10% O<sub>2</sub>, 40% N<sub>2</sub>, 8% CO<sub>2</sub>, 41% H<sub>2</sub>), no significant distinctions emerge in the development process and gas uptake (**Fig. 8a**). The presence of 41% H<sub>2</sub> also allows the culture without N compounds to maintain itself in linear growth (**Fig. 8a**). However, in the modified atmosphere condition (10% O<sub>2</sub>, 71% N<sub>2</sub>, 8% CO<sub>2</sub>, 10% H<sub>2</sub>), the first 48 hours of growth seems to show similar behaviours between the two cultures, but thereafter a differentiation becomes apparent from 72 hours onward (**Fig. 11a**). It should be emphasised that although a thorough statistical evaluation between the two samples might be necessary, the currently available data do not allow a reliable conclusion. In any case, it is plausible to speculate that the lower presence of H<sub>2</sub> and the absence of N compounds may induce greater stress than the other conditions considered and an increase in PHB accumulation (Sun et al., 2020; Ahn et al. 2015). An interesting option would be to extend the duration of the experiment to see if the differences become more pronounced over time. It can also be observed that CO<sub>2</sub> consumption remains comparable across N conditions (**Fig. 8b**), indicating similar assimilation over time. As regards H<sub>2</sub>, the volumes input to cultures vary according to the atmosphere adopted, but it is evident that nutrient deficiency does not affect H<sub>2</sub> consumption (**Fig. 8c**). At the end of the experiment (after seven days), samples were collected for PHB analysis. However, due to technical difficulties, these samples were

not sent for analysis in a timely manner, making a complete assessment of the starvation situation impossible at the moment.

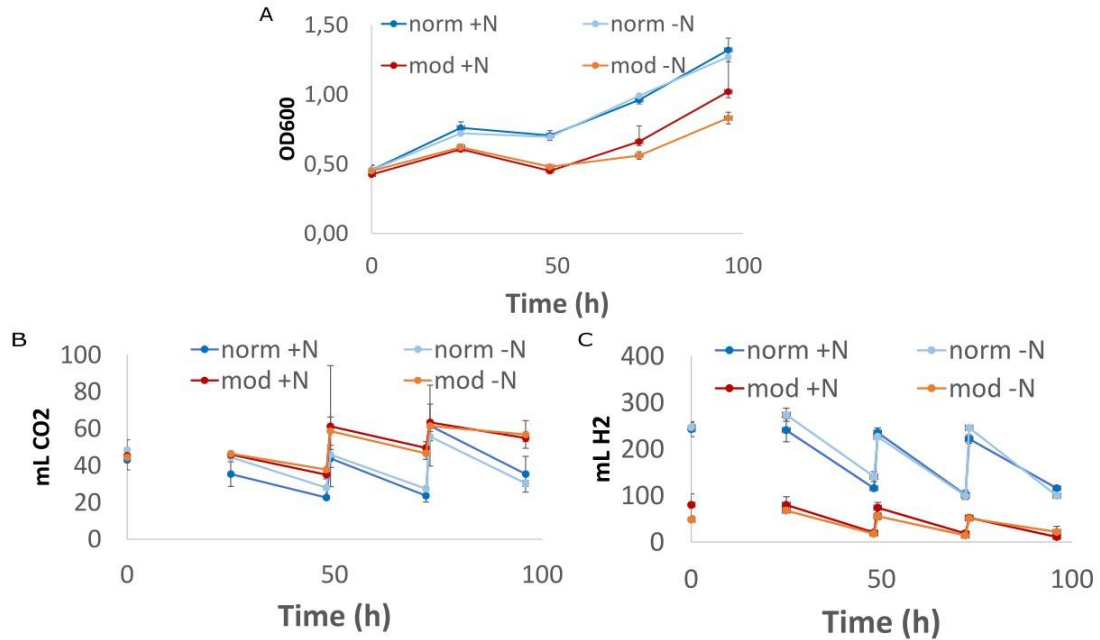


**Figure 8.** Growth trend among four different conditions (a); CO<sub>2</sub> consumption trend (b); H<sub>2</sub> consumption trend (c).

### 3.4. Metabolic changes in *C. necator* upon chemolithotrophic growth

#### 3.4.1. Comparison between adapted and not adapted conditions

In order to confirm the results obtained in the first experiment with small bottles, the experiment was replicated using 550 mL bottles. After 24 hours from the start of the experiment, a sample was taken from each bottle for transcriptomic analysis. The main objective of this analysis was to identify any noticeable differences at the transcriptomic level between the CO<sub>2</sub>-adapted and non-adapted cultures. The aim of examining the transcriptome was to gain insights into the gene expression patterns and potential regulatory changes induced by CO<sub>2</sub> adaptation in *C. necator*.

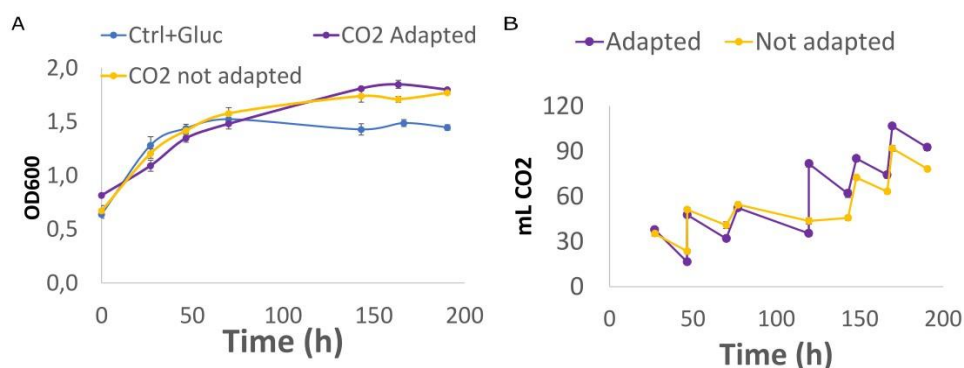


**Figure 9.** Growth trend (a) and CO<sub>2</sub> consumption (b) among not adapted and adapted conditions.

The experiment was conducted over nine days and the results show substantial homogeneity in both the growth trends (**Fig. 9a**) and CO<sub>2</sub> assimilation between the different conditions (**Fig. 9b**). It is remarkable that in the early stages, the CO<sub>2</sub> trend for the unadapted condition coincides with that of the glucose-containing control. In fact, both follow an exponential trend in the first 24 hours, probably as a consequence of the residual consumption of glucose from the inoculum. Furthermore, it is interesting to note that CO<sub>2</sub> uptake in the adapted condition is more efficient than in the not adapted condition, the distinction between the two conditions becomes even more pronounced after about 100 hours, with the curve for the adapted condition showing a significant increase in CO<sub>2</sub> uptake compared to the unadapted condition..

### 3.4.2. Adaptation phase – PHB accumulation analysis

Regarding the samples from which aliquots were taken for transcriptomic analysis, it is worth mentioning that samples were collected for PHB extraction at the end of the experiment (after nine days). Interestingly, for both the samples undergoing adaptation and those already adapted, no differences in PHB values were found, but it is not possible to conclude with certainty that these differences may be significant (p-value 0.06). This result suggests that neither the duration of adaptation nor the conditions themselves seem to have had a major impact on polymer accumulation in the cultures (**Fig. D1** in **Appendix Section D**).

The evolution over time of the utilisation of the accumulated granules is not clearly defined; however, it is reasonable to assume that *C. necator* assimilated CO<sub>2</sub> when it was available, using the later synthesised granules when CO<sub>2</sub> levels begin to decline in the culture headspace. This assumption reflects the possibility that the bacterium used PHB granules as a carbon reserve when the CO<sub>2</sub> source gets limiting.

### 3.4.3. Overview of transcriptional profiles

In the research conducted by Amer and Kim (2023), it was verified that *C. necator* is able to make the transition between autotrophic and heterotrophic metabolism, and vice versa, within a 12-hour time interval. Analysis of the *C. necator* transcriptome revealed relevant disparities between the two conditions considered (prior adaptation to CO<sub>2</sub> or lack thereof). Both the CO<sub>2</sub> adapted and unadapted conditions were compared to glucose, which served as the control. Overall, the unadapted samples show similarities with the glucose-cultivated ones. This is reflected in the cell growth data, where the trend between the two conditions is virtually identical in the first 24 hours. This result supports the previous observation that residual glucose may still be present and that the metabolism is starting to shift. However, there is a set of upregulated genes that is also upregulated in the CO<sub>2</sub>-adapted condition, showing that 24 hours after inoculation, even if glucose is probably present in the medium in small amounts, the metabolism is already changing. Interestingly, 26 genes are only differentially expressed in unadapted samples (**Fig. 10**). This suggests that the transition from heterotrophic to autotrophic condition may involve the transient activation of some genes which may no longer be needed in the adapted condition. The adapted condition, in contrast, had a remarkable number of genes which were differentially expressed with respect to the control, indicating a deep change in the metabolic state of the cells (**Fig. 10**). Specifically, 365 genes were identified for the CO<sub>2</sub> adapted, while only 61 for the CO<sub>2</sub> non-adapted. This disparity in the amount of differentially expressed genes highlights the important impact of CO<sub>2</sub> adaptation on the transcriptome of *C. necator*.

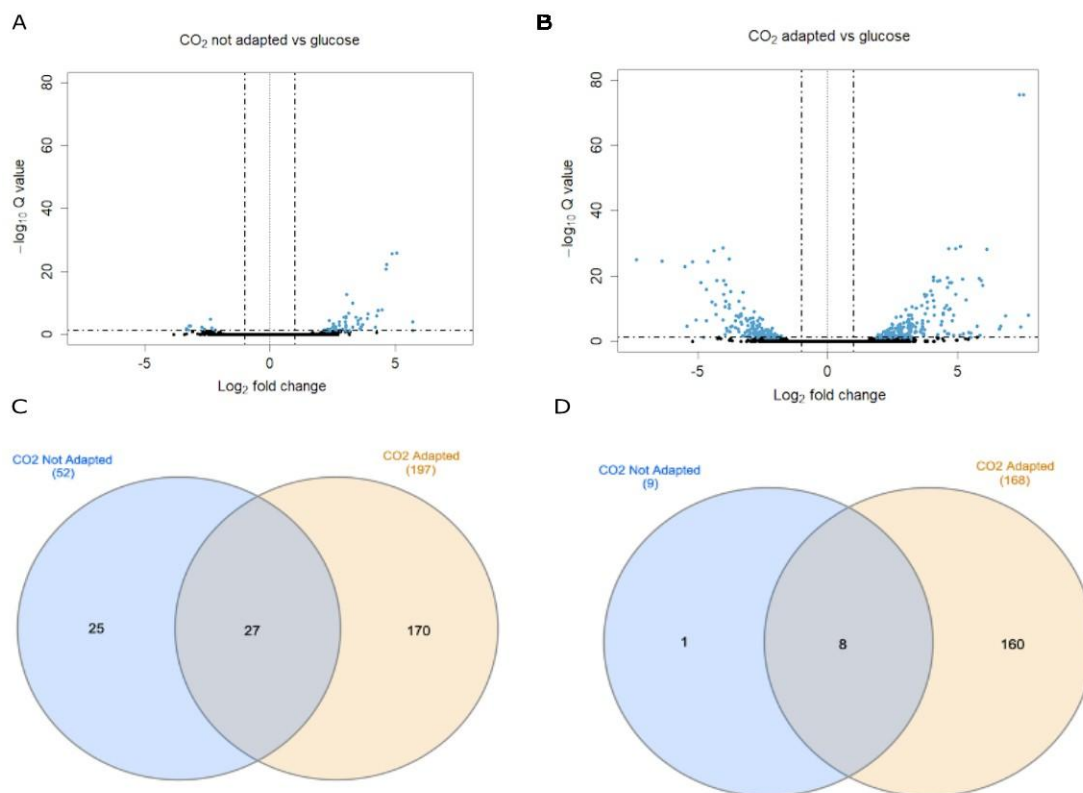


**Figure 10.** Volcano plots showing differentially expressed genes in CO<sub>2</sub>-not adapted (a) and CO<sub>2</sub>-adapted (b) conditions. Q-value threshold = 0.05, log-fold change threshold = ±1. Venn diagrams comparing sets of significantly upregulated (c) and downregulated (d) genes in CO<sub>2</sub>-not adapted and CO<sub>2</sub>-adapted conditions.

Referring to the Kohlmann et al. (2011) study, which involved a proteomic analysis comparing heterotrophic and lithoautotrophic conditions, the latter showcased predominant expression of three main functional groups: energy production/conversion processes, transport functions and CO<sub>2</sub> fixation. Results from the present work generally agree with those obtained in the proteomic study. Some of the most highly expressed genes in the adapted condition encode enzymes involved in energy metabolism and ABC transporters. While in the study by Kohlmann et al. (2011) most of these transporters were of the HAAT and PAAT type involved in amino acid uptake, this work revealed different transporter types, notably those involved in phosphate assimilation. The increased expression of ABC-type

transporters could be attributed to an enhanced requirement of inorganic compounds during autotrophic growth (**Table E1 in Appendix Section E**).

There is a high level of expression of the accessory proteins HypC and HypB (**Fig. 11**), which are required in the maturation and incorporation of the cofactor [Ni-Fe] into apo-hydrogenase (Forzi and Sawers 2007; Lacasse and Zamble 2016). As expected, once the organism was cultured in the presence of H<sub>2</sub>, its requirement for H<sub>2</sub>-oxidising enzymes was much higher.

Another expected finding concerned the increased expression of genes involved in CBB, among these genes are those involved in the formation of RuBiSCO, such as those involved in the synthesis of large and small chains (see **Table E1 in Appendix Section E**). This could be explained as growth in the presence of H<sub>2</sub>/CO<sub>2</sub> requires the activation of CBB enzymes that are encoded in two clusters, one located on chromosome 2 and the other on the pHG1 megaplasmid (Kohlmann et al. 2011). This result further emphasises the crucial importance of these metabolic pathways in the adaptation of the organism to autotrophic growth conditions. Other upregulated genes were involved in amino acid synthesis, such as valine, leucine and isoleucine (**Table E1 in Appendix Section E**). In addition, a number of downregulated genes have been identified (**Table E4 in Appendix Section E**), including those involved in the formation of ATP synthase, in particular the beta subunit, and some genes involved in the formation of NADH quinone oxidoreductase. The latter is a class I NADH dehydrogenase responsible for introducing electrons generated by the oxidation of NADH into the electron chain by reducing the quinone pool (Kohlmann et al., 2011). In *C. necator*, this enzyme is encoded by 14 genes (*nuoA-nuoN*) and its downregulation suggests the possibility that the organism is adopting an alternative strategy for NADH oxidation (Kohlmann et al., 2011). Regarding PHB production, a significant increase in the expression of the gene H16\_B2349, which codes for a sigma factor activator 54, was observed. This factor plays a key role in PHB granule synthesis (Hoffmann and Rehm 2004; Rehm 2006). Interestingly, a lower expression was observed for the genes H16\_A1438 and H16\_A1439, which code for acetyl-CoA acetyltransferase (PhaA) and acetoacetyl-CoA reductase (PhaB1), respectively. Previous research has shown that expression levels of the phaC1AB1 operon

remained constant under stress-free conditions and increased in response to low-N stress (Shimizu et al. 2013). It could be that the basal expression of the *phaCAB* operon is lower in lithoautotrophic conditions, albeit stress-free, since carbon fixation is an energetically demanding process. However, this aspect needs to be clarified with further experiments involving nutritional stresses in autotrophic conditions.

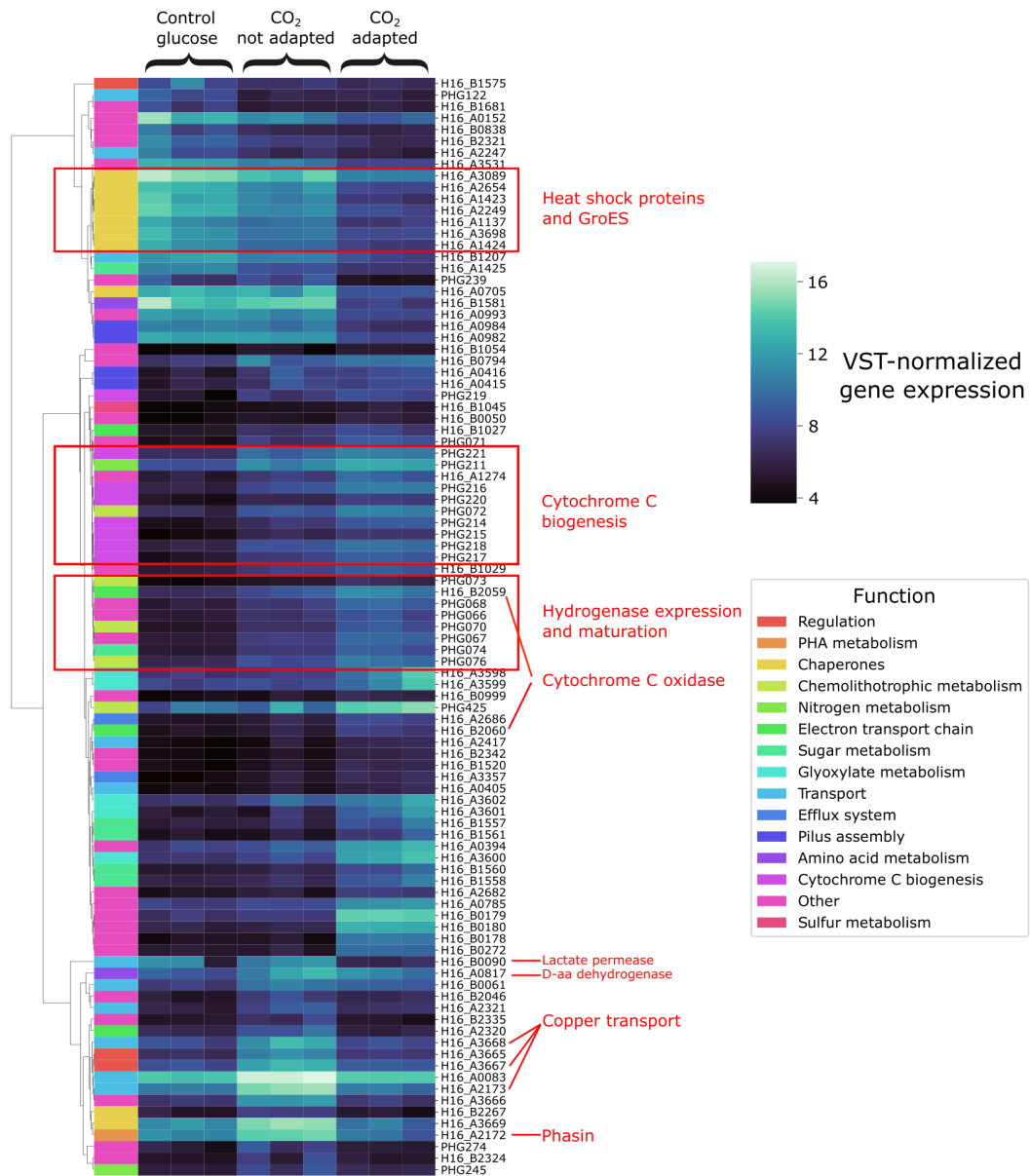


**Figure 11.** Heat map of expression values for a set of 95 significant and highly variable (LFC > 3) genes in the three different conditions



As mentioned before, the CO<sub>2</sub> unadapted condition was characterised by the upregulation of some genes which were not found as significantly overexpressed in CO<sub>2</sub> adapted samples (see **Table E3** in **Appendix Section E**). Among these genes, those involved in the synthesis and regulation of copper transporters were identified, which confer increased resistance to this metal (Shimizu et al. 2013). The increased expression of these genes during the adaptation process can be explained by the formation of certain active copper-containing enzymes, such as cytochrome c oxidase, which play an essential role in the respiratory chain (Michel et al. 1998). Remarkably, an increase in the expression of the H16\_A2172 gene, responsible for encoding PhaP3, a protein known as phasin, was observed. Phasins are structural proteins which coat PHB granules once they have been synthesised (Pötter et al. 2002). The different regulation of these genes between not adapted and adapted conditions could be attributable to the variation in PHB granule formation in the two situations. These results further solidify the idea that the transition from heterotrophic to lithoautotrophic metabolism is a complex process which probably involves an intermediate phase where some genes are transiently expressed. Further investigation, such as a time-course experiment, is needed to thoroughly describe this transition.

## 4. Conclusions

The analysis conducted clearly showed the extraordinary metabolic versatility of *C. necator*. During autotrophic growth, it exhibited constant growth and the scale-up process did not seem to significantly influence the yield. It was also found that without the introduction of nutrient deficiency stress, PHB accumulation rates do not reach high levels, as expected. The input of gases such as H<sub>2</sub>, O<sub>2</sub> and CO<sub>2</sub> was found to be a limiting factor, and there is a need to explore new approaches for mixing and optimising gas/liquid exchange to improve the efficiency of the CO<sub>2</sub> fixation. An additional observation concerns the significant H<sub>2</sub> requirements for autotrophic growth, which could yield considerable increases in production costs if the process were to be industrialised. With the supply of VFA, *C. necator* growth did not reach high values and that the carbon concentration had a significant influence on the growth curve, both at low and high concentrations. However, the use of VFA is an intriguing approach, as it allows the use of waste materials and the synthesis of copolymers with different compositions, thus enhancing the properties of the resulting products. A more in-depth study of the composition of VFA and the identification of the most promising acids as substrates could lead to a significant increase in the production of copolymers of interest, thus, more experiments with pH control will be needed in the future.

In the context of nutrient deficiency, the data obtained suggest a significant increase in the accumulation of PHA. It would be particularly interesting to conduct further evaluation after actual PHA extraction in order to establish a clear correlation between Nile-Red fluorescence and polymer accumulation through gas chromatography measurements in a time course specific study. In addition, a more detailed analysis of C/N ratios could reveal new opportunities to optimise PHA accumulation, thereby improving the yield of the process. It became evident that the lack of phosphate in the culture medium was an extremely limiting factor for the growth of *C. necator*.

Finally, transcriptomic analysis revealed an interesting pattern regarding the gene expression of *C. necator* under the different conditions examined. Results obtained in the current study confirm the remarkable metabolic flexibility of *C. necator* and its ability to adapt to various environmental conditions, these results further solidify the idea that the transition from heterotrophic to lithoautotrophic metabolism is a complex progression which probably involves an intermediate phase where some genes are transiently expressed. Further analysis, especially under nutrient-deficient conditions, could contribute to a deeper understanding of the genes involved in PHA granule synthesis, leading to a detailed characterization of the metabolic profiles and pathways expressed. Transcriptomics studies could also reveal the key genes involved in the pathways of interest, opening up new opportunities in the field of genetic engineering and enabling optimization of the PHA production yield.

## 5. References

Ahn, Junmo, Eun Hea Jho, and Kyoungphile Nam. 'Effect of C/N Ratio on Polyhydroxyalkanoates (PHA) Accumulation by *Cupriavidus Necator* and Its Implication on the Use of Rice Straw Hydrolysates'. *Environmental Engineering Research* 20, no. 3 (30 September 2015): 246–53. <https://doi.org/10.4491/eer.2015.055>.

Amer, Abdelrahman, and Younggy Kim. 'Minimising the Lag Phase of *Cupriavidus Necator* Growth under Autotrophic, Heterotrophic, and Mixotrophic Conditions'. Edited by Pablo Ivan Nikel. *Applied and Environmental Microbiology* 89, no. 2 (28 February 2023): e02007-22. <https://doi.org/10.1128/aem.02007-22>.

Bellini, Silvia, Tonia Tommasi, and Debora Fino. 'Poly(3-Hydroxybutyrate) Biosynthesis by *Cupriavidus Necator*: A Review on Waste Substrates Utilisation for a Circular Economy Approach'. *Bioresource Technology Reports* 17 (February 2022): 100985. <https://doi.org/10.1016/j.biteb.2022.100985>.

Bowien, B, and H G Schlegel. 'Physiology and Biochemistry of Aerobic Hydrogen-Oxidizing Bacteria'. *Annual Review of Microbiology* 35, no. 1 (October 1981): 405–52. <https://doi.org/10.1146/annurev.mi.35.100181.002201>.

Brandll, Helmut, and Richard A Gross. 'Plastics from Bacteria and for Bacteria: Poly([I-Hydroxy- Alkanoates) as Natural, Biocompatible, and Biodegradable Polyesters', n.d.

Braunegg, G., B. Sonnleitner, and R. M. Lafferty. 'A Rapid Gas Chromatographic Method for the Determination of Poly-?-Hydroxybutyric Acid in Microbial Biomass'. *European Journal of Applied Microbiology and Biotechnology* 6, no. 1 (1978): 29–37. <https://doi.org/10.1007/BF00500854>.

Bugnicourt, E., P. Cinelli, A. Lazzeri, and V. Alvarez. 'Polyhydroxyalkanoate (PHA): Review of Synthesis, Characteristics, Processing and Potential Applications in Packaging'. *Express Polymer Letters* 8, no. 11 (2014): 791–808. <https://doi.org/10.3144/expresspolymlett.2014.82>.

Castro-Sowinski, Susana, Saul Burdman, Ofra Matan, and Yaacov Okon. 'Natural Functions of Bacterial Polyhydroxyalkanoates'. In *Plastics from Bacteria*, edited by George Guo-Qiang Chen, 14:39–61. Microbiology Monographs. Berlin, Heidelberg: Springer Berlin Heidelberg, 2010. [https://doi.org/10.1007/978-3-642-03287-5\\_3](https://doi.org/10.1007/978-3-642-03287-5_3).

Choi, Jong-il, and Sang Yup Lee. 'Process Analysis and Economic Evaluation for Poly(3-Hydroxybutyrate) Production by Fermentation'. *Bioprocess Engineering* 17, no. 6 (1997): 335. <https://doi.org/10.1007/s004490050394>.

Forzi, Lucia, and R Gary Sawers. 'Maturation of [NiFe]-Hydrogenases in *Escherichia Coli*', 2007.

Garcia-Gonzalez, Linsey, Md. Salatul Islam Mozumder, Majorie Dubreuil, Eveline I.P. Volcke, and Heleen De Wever. 'Sustainable Autotrophic Production of Polyhydroxybutyrate (PHB) from CO<sub>2</sub> Using a Two-Stage Cultivation System'. *Catalysis Today* 257 (November 2015): 237–45. <https://doi.org/10.1016/j.cattod.2014.05.025>.

Hoffmann, Nils, and Bernd H.A. Rehm. 'Regulation of Polyhydroxyalkanoate Biosynthesis in *Pseudomonas Putida* and *Pseudomonas Aeruginosa*'. *FEMS Microbiology Letters* 237, no. 1 (August 2004): 1–7. <https://doi.org/10.1111/j.1574-6968.2004.tb09671.x>.

Horvat, Predrag, Ivna Vrana Špoljarić, Markan Lopar, Aid Atlić, Martin Koller, and Gerhart Braunegg. 'Mathematical Modelling and Process Optimization of a Continuous 5-Stage Bioreactor Cascade for Production of

Poly[-(R)-3-Hydroxybutyrate] by *Cupriavidus Necator*'. *Bioprocess and Biosystems Engineering* 36, no. 9 (September 2013): 1235–50. <https://doi.org/10.1007/s00449-012-0852-8>.

A. Ishizaki, K. Tanaka, T. Takeshita, T. Kanemaru, T. Shimoji, T. Kawano, J. Chem. Eng. Jpn. 26 (1993) 225–227.

Jawed, Kamran, Victor Uzunoma Irorere, Rajesh Reddy Bommareddy, Nigel P. Minton, and Katalin Kovács. 'Establishing Mixotrophic Growth of *Cupriavidus Necator* H16 on CO<sub>2</sub> and Volatile Fatty Acids'. *Fermentation* 8, no. 3 (14 March 2022): 125. <https://doi.org/10.3390/fermentation8030125>.

Jendrossek, Dieter. 'Polyhydroxyalkanoate Granules Are Complex Subcellular Organelles (Carbonosomes)'. *Journal of Bacteriology* 191, no. 10 (15 May 2009): 3195–3202. <https://doi.org/10.1128/JB.01723-08>.

Kedia, Gopal, Pearl Passanha, Richard M. Dinsdale, Alan J. Guwy, and Sandra R. Esteves. 'Evaluation of Feeding Regimes to Enhance PHA Production Using Acetic and Butyric Acids by a Pure Culture of *Cupriavidus Necator*'. *Biotechnology and Bioprocess Engineering* 19, no. 6 (November 2014): 989–95. <https://doi.org/10.1007/s12257-014-0144-z>.

Khanna, Shilpi, and Ashok K. Srivastava. 'Recent Advances in Microbial Polyhydroxyalkanoates'. *Process Biochemistry* 40, no. 2 (February 2005): 607–19. <https://doi.org/10.1016/j.procbio.2004.01.053>.

Kim, Soyoung, Yong Jae Jang, Gyeongtaek Gong, Sun-Mi Lee, Youngsoon Um, Kyoung Heon Kim, and Ja Kyong Ko. 'Engineering *Cupriavidus Necator* H16 for Enhanced Lithoautotrophic Poly(3-Hydroxybutyrate) Production from CO<sub>2</sub>'. *Microbial Cell Factories* 21, no. 1 (5 November 2022): 231. <https://doi.org/10.1186/s12934-022-01962-7>.

Kohlmann, Yvonne, Anne Pohlmann, Andreas Otto, Dörte Becher, Rainer Cramm, Steffen Lütte, Edward Schwartz, Michael Hecker, and Bärbel Friedrich. ‘Analyses of Soluble and Membrane Proteomes of *Ralstonia Eutropha* H16 Reveal Major Changes in the Protein Complement in Adaptation to Lithoautotrophy’. *Journal of Proteome Research* 10, no. 6 (3 June 2011): 2767–76. <https://doi.org/10.1021/pr101289v>.

König, C., Sammler, I., Wilde, E., Schlegel, H.G., 1969. Konstitutive Glucose-6-phosphat-Dehydrogenase bei Glucose verwertenden Mutanten von einem kryptischen Wildstamm [Constitutive glucose-6-phosphate dehydrogenase in mutants utilizing glucose, which are derived from cryptic wildtype strains]. *Arch. Mikrobiol.* 67, 51–57.

Lacasse, Michael J., and Deborah B. Zamble. ‘[NiFe]-Hydrogenase Maturation’. *Biochemistry* 55, no. 12 (29 March 2016): 1689–1701. <https://doi.org/10.1021/acs.biochem.5b01328>.

Lenz, Robert W., and Robert H. Marchessault. ‘Bacterial Polyesters: Biosynthesis, Biodegradable Plastics and Biotechnology’. *Biomacromolecules* 6, no. 1 (1 January 2005): 1–8. <https://doi.org/10.1021/bm049700c>.

Lu, Yue, and Jian Yu. ‘Comparison Analysis on the Energy Efficiencies and Biomass Yields in Microbial CO<sub>2</sub> Fixation’. *Process Biochemistry* 62 (November 2017): 151–60. <https://doi.org/10.1016/j.procbio.2017.07.007>.

Meereboer, Kjeld W., Manjusri Misra, and Amar K. Mohanty. ‘Review of Recent Advances in the Biodegradability of Polyhydroxyalkanoate (PHA) Bioplastics and Their Composites’. *Green Chemistry* 22, no. 17 (2020): 5519–58. <https://doi.org/10.1039/D0GC01647K>.

Michel, H., J. Behr, A. Harrenga, and A. Kannt. 'CYTOCHROME C OXIDASE: Structure and Spectroscopy'. *Annual Review of Biophysics and Biomolecular Structure* 27, no. 1 (June 1998): 329–56. <https://doi.org/10.1146/annurev.biophys.27.1.329>.

Mozumder, Md. Salatul Islam, Heleen De Wever, Eveline I.P. Volcke, and Linsey Garcia-Gonzalez. 'A Robust Fed-Batch Feeding Strategy Independent of the Carbon Source for Optimal Polyhydroxybutyrate Production'. *Process Biochemistry* 49, no. 3 (March 2014): 365–73. <https://doi.org/10.1016/j.procbio.2013.12.004>.

Obruca, S., I. Marova, Z. Svoboda, and R. Mikulikova. 'Use of Controlled Exogenous Stress for Improvement of Poly(3-Hydroxybutyrate) Production in *Cupriavidus Necator*'. *Folia Microbiologica* 55, no. 1 (January 2010): 17–22. <https://doi.org/10.1007/s12223-010-0003-z>.

Pearcy, N., Garavaglia, M., Millat, T., Gilbert, J.P., Song, Y., Hartman, H., Woods, C., Tomi-Andrino, C., Bommareddy, R.R., Cho, B.-K., Fell, D.A., Poolman, M., King, J.R., Winzer, K., Twycross, J., Minton, N.P., 2022. A genome-scale metabolic model of *Cupriavidus necator* H16 integrated with TraDIS and transcriptomic data reveals metabolic insights for biotechnological applications. *PLOS Comput. Biol.* 18, e1010106. <https://doi.org/10.1371/journal.pcbi.1010106>

Pohlmann, Anne, Rainer Cramm, Karin Schmelz, and Bärbel Friedrich. 'A Novel NO-Responding Regulator Controls the Reduction of Nitric Oxide in *Ralstonia Eutropha*'. *Molecular Microbiology* 38, no. 3 (November 2000): 626–38. <https://doi.org/10.1046/j.1365-2958.2000.02157.x>.

Pötter, Markus, Mohamed H. Madkour, Frank Mayer, and Alexander Steinbüchel. 'Regulation of Phasin Expression and Polyhydroxyalkanoate (PHA) Granule Formation in *Ralstonia Eutropha* H16'. *Microbiology* 148, no. 8 (1 August 2002): 2413–26. <https://doi.org/10.1099/00221287-148-8-2413>.



Preusting, Hans, Atze Nijenhuis, and Bernard Witholt. 'Physical Characteristics of Poly(3-Hydroxyalkanoates) and Poly(3-Hydroxyalkenoates) Produced by Pseudomonas Oleovorans Grown on Aliphatic Hydrocarbons'. *Macromolecules* 23, no. 19 (September 1990): 4220–24. <https://doi.org/10.1021/ma00221a007>.

Raberg, Matthias, Katja Peplinski, Silvia Heiss, Armin Ehrenreich, Birgit Voigt, Christina Döring, Mechthild Bömeke, Michael Hecker, and Alexander Steinbüchel. 'Proteomic and Transcriptomic Elucidation of the Mutant *Ralstonia Eutropha* G<sup>+</sup> 1 with Regard to Glucose Utilization'. *Applied and Environmental Microbiology* 77, no. 6 (15 March 2011): 2058–70. <https://doi.org/10.1128/AEM.02015-10>.

Rehm, Bernd H. A. 'Genetics and Biochemistry of Polyhydroxyalkanoate Granule Self-Assembly: The Key Role of Polyester Synthases'. *Biotechnology Letters* 28, no. 4 (February 2006): 207–13. <https://doi.org/10.1007/s10529-005-5521-4>.

Ryu H.-W., Cho K.-S., Kim B.-S., Chang Y.-K., Chang H.-N., Shim H.-J. (1999). Mass Production of Poly(3-Hydroxybutyrate) by Fed-Batch Cultures of *Ralstonia Eutropha* with Nitrogen and Phosphate Limitation. *J. Microbiol. Biotechnol.* 9 (6), 751–756.

Sauer, U., Canonaco, F., Heri, S., Perrenoud, A., Fischer, E., 2004. The soluble and membrane-bound transhydrogenases UdhA and PntAB have divergent functions in NADPH metabolism of *Escherichia coli*. *J. Biol. Chem.* 279, 6613–6619. <https://doi.org/10.1074/jbc.M311657200>.

Schröder, V., B. Emonts, H. Janßen, and H.-P. Schulze. 'Explosion Limits of Hydrogen/Oxygen Mixtures at Initial Pressures up to 200 Bar'. *Chemical Engineering & Technology* 27, no. 8 (August 2004): 847–51. <https://doi.org/10.1002/ceat.200403174>.

Shen, Li, Juliane Haufe, and Martin K Patel. 'June 2009 Revised in Novmeber 2009', n.d.

Sheu, D.-S., W.-M. Chen, Y.-W. Lai, and R.-C. Chang. 'Mutations Derived from the Thermophilic Polyhydroxyalkanoate Synthase PhaC Enhance the Thermostability and Activity of PhaC from *Cupriavidus Necator* H16'. *Journal of Bacteriology* 194, no. 10 (15 May 2012): 2620–29. <https://doi.org/10.1128/JB.06543-11>.

Shimizu, Rie, Kenta Chou, Izumi Orita, Yutaka Suzuki, Satoshi Nakamura, and Toshiaki Fukui. 'Detection of Phase-Dependent Transcriptomic Changes and Rubisco-Mediated CO<sub>2</sub> Fixation into Poly (3-Hydroxybutyrate) under Heterotrophic Condition in *Ralstonia Eutropha* H16 Based on RNA-Seq and Gene Deletion Analyses'. *BMC Microbiology* 13, no. 1 (December 2013): 169. <https://doi.org/10.1186/1471-2180-13-169>.

Sirohi, Ranjna, Jai Prakash Pandey, Vivek Kumar Gaur, Edgard Gnansounou, and Raveendran Sindhu. 'Critical Overview of Biomass Feedstocks as Sustainable Substrates for the Production of Polyhydroxybutyrate (PHB)'. *Bioresource Technology* 311 (September 2020): 123536. <https://doi.org/10.1016/j.biortech.2020.123536>.

Spaans, S., Weusthuis, R., Van Der Oost, J., Kengen, S., 2015. NADPH-generating systems in bacteria and archaea. *Front. Microbiol.* 6.

Spiekermann, Patricia, Bernd H. A. Rehm, Rainer Kalscheuer, Dirk Baumeister, and A. Steinbüchel. 'A Sensitive, Viable-Colony Staining Method Using Nile Red for Direct Screening of Bacteria That Accumulate Polyhydroxyalkanoic Acids and Other Lipid Storage Compounds'. *Archives of Microbiology* 171, no. 2 (14 January 1999): 73–80. <https://doi.org/10.1007/s002030050681>.

T. Takeshita, A. Ishizaki, J. Ferment. Bioeng. 81 (1996) 83–86.

Tiemeyer, Armin, Hannes Link, and Dirk Weuster-Botz. ‘Kinetic Studies on Autohydrogenotrophic Growth of *Ralstonia Eutropha* with Nitrate as Terminal Electron Acceptor’. *Applied Microbiology and Biotechnology* 76, no. 1 (August 2007): 75–81. <https://doi.org/10.1007/s00253-007-0983-z>.

Tokiwa, Yutaka, Buenaventurada Calabia, Charles Ugwu, and Seiichi Aiba. ‘Biodegradability of Plastics’. *International Journal of Molecular Sciences* 10, no. 9 (26 August 2009): 3722–42. <https://doi.org/10.3390/ijms10093722>.

Vu, Danh H., Amir Mahboubi, Andrew Root, Ivo Heinmaa, Mohammad J. Taherzadeh, and Dan Åkesson. ‘Thorough Investigation of the Effects of Cultivation Factors on Polyhydroalkanoates (PHAs) Production by *Cupriavidus Necator* from Food Waste-Derived Volatile Fatty Acids’. *Fermentation* 8, no. 11 (4 November 2022): 605. <https://doi.org/10.3390/fermentation8110605>.

Wang, Jin, Zheng-Bo Yue, Guo-Ping Sheng, and Han-Qing Yu. ‘Kinetic Analysis on the Production of Polyhydroxyalkanoates from Volatile Fatty Acids by *Cupriavidus Necator* with a Consideration of Substrate Inhibition, Cell Growth, Maintenance, and Product Formation’. *Biochemical Engineering Journal* 49, no. 3 (May 2010): 422–28. <https://doi.org/10.1016/j.bej.2010.02.005>.

Yeo, Jayven Chee Chuan, Joseph K. Muiruri, Warintorn Thitsartarn, Zibiao Li, and Chaobin He. ‘Recent Advances in the Development of Biodegradable PHB-Based Toughening Materials: Approaches, Advantages and Applications’. *Materials Science and Engineering: C* 92 (November 2018): 1092–1116. <https://doi.org/10.1016/j.msec.2017.11.006>.

Yu, Jian, and Pradeep Munasinghe. 'Gas Fermentation Enhancement for Chemolithotrophic Growth of *Cupriavidus Necator* on Carbon Dioxide'. *Fermentation* 4, no. 3 (9 August 2018): 63. <https://doi.org/10.3390/fermentation4030063>.

Yu, Jian, Yingtao Si, Wan Keung, and R. Wong. 'Kinetics Modeling of Inhibition and Utilization of Mixed Volatile Fatty Acids in the Formation of Polyhydroxyalkanoates by *Ralstonia Eutropha*'. *Process Biochemistry* 37, no. 7 (February 2002): 731–38. [https://doi.org/10.1016/S0032-9592\(01\)00264-3](https://doi.org/10.1016/S0032-9592(01)00264-3).

## 6. Appendix

### 6.1. Appendix A - medium 81 recipe

**Table A1.** Medium 81 for chemolithotrophic growth

<b>Solution A</b>	KH <sub>2</sub> PO <sub>4</sub> 2,300 g Na <sub>2</sub> HPO <sub>4</sub> x 2 H <sub>2</sub> O 2,900 g Distilled water 50,000 mL
<b>Solution B</b>	NH <sub>4</sub> Cl 1,000 g MgSO <sub>4</sub> x 7 H <sub>2</sub> O 0,500 g CaCl <sub>2</sub> x 2 H <sub>2</sub> O 0,010 g MnCl <sub>2</sub> x 4 H <sub>2</sub> O 0,005 g NaVO <sub>3</sub> x H <sub>2</sub> O 0,005 g Distilled water 915 mL Agar (if necessary) 20,000 g
<b>Solution C</b>	Ferric ammonium citrate 0,050 g Distilled water 20,000 mL

<b>Microelement solutions</b>	ZnSO <sub>4</sub> x 7H <sub>2</sub> O 0.1 g/L  MnCl <sub>2</sub> x 4H <sub>2</sub> O 0.03 g/L  H <sub>3</sub> BO <sub>3</sub> 0.3 g/L
-------------------------------	---

	<p>CoCl<sub>2</sub> x 6H<sub>2</sub>O 0.2 g/L</p> <p>CuCl<sub>2</sub> x 2H<sub>2</sub>O 0.01 g/L</p> <p>NiCl<sub>2</sub> x 6H<sub>2</sub>O 0.02 g/L</p> <p>NaMoO<sub>4</sub> x 2H<sub>2</sub>O 0.03 g/L</p>
--	---

<b>Standard vitamin solution</b>	<p>Riboflavin 0.5 mg/L</p> <p>Thiamine-HCl x 2H<sub>2</sub>O 0.5 mg/L</p> <p>Nicotinic acid 0.5 mg/L</p> <p>Pyridoxine-HCl 1 mg/L</p> <p>Ca-pantothenate 0.5 mg/L</p> <p>Biotin 0.2 mg/L</p> <p>Folic acid 0.2 mg/L</p> <p>Vitamin B12 0.01 mg/L</p> <p>Lipoic acid 0.5 mg/L</p> <p>P-aminobenzoic acid 0.5 mg/L</p>
----------------------------------	--

## 6.2. Appendix B - VFA content

**Table B1.** VFA content in the VFA mixture

Formic acid	HCOOH
Acetic acid	CH <sub>3</sub> COOH
Propionic acid	CH <sub>3</sub> CH <sub>2</sub> COOH
Butyric acid	CH <sub>3</sub> CH <sub>2</sub> CH <sub>2</sub> COOH
Isobutyric acid	(CH <sub>3</sub> ) <sub>2</sub> CHCOOH
Valeric acid	CH <sub>3</sub> (CH <sub>2</sub> ) <sub>3</sub> COOH
Isovaleric acid	(CH <sub>3</sub> ) <sub>2</sub> CHCH <sub>2</sub> COOH
Isocaproic acid (4-methyl-valeric acid)	(CH <sub>3</sub> ) <sub>2</sub> CHCH <sub>2</sub> CH <sub>2</sub> COOH
Hexanoic acid	CH <sub>3</sub> (CH <sub>2</sub> ) <sub>4</sub> COOH
Heptanoic acid	CH <sub>3</sub> (CH <sub>2</sub> ) <sub>5</sub> COOH

### 6.3. Appendix C - N starvation

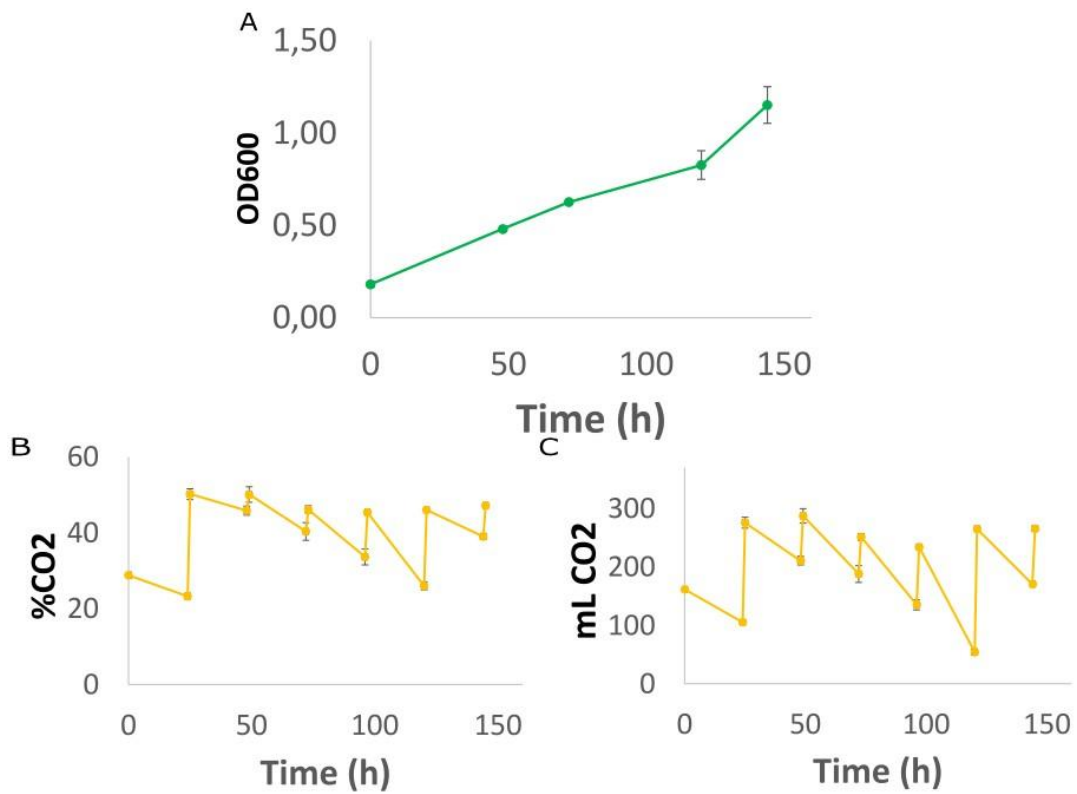


**Figure C1.** Growth trend during adaptation phase and CO<sub>2</sub> consumption trend

### 6.4. Appendix D - PHB

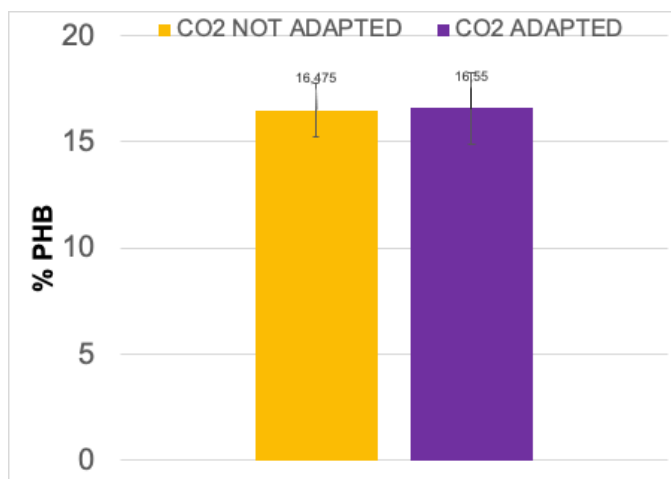


**Figure D1.** PHB accumulation percentage among not adapted and adapted conditions



## 6.5. Appendix E - Genes table

**Table E1.** Upregulated genes Adapted condition

Gene	KEGG code	Log2 Fold Change	Function	Pathway
H16_A24 41	K02036	2,47	ABC-type phosphate transport system ATP-binding protein	ABC transportes
H16_A24 42	K02038	3,63	phosphate transport system permease protein   (GenBank) pstA; ABC-type transporter, permease protein	
H16_A24 43	K02037	3,56	phosphate transport system permease protein   (GenBank) pstC; ABC-type transporter, permease protein	
H16_A36 00	K00042	6,10	2-hydroxy-3-oxopropionate reductase [EC: <a href="#">1.1.1.60</a> ]   (GenBank) h16_A3600; 2-hydroxy-3-oxopropionate reductase	Carbohydrate metabolism

H16_A36 01	K11529	6,60	glycerate 2-kinase [EC: <a href="#">2.7.1.165</a> ]   (GenBank) ttuD1; glycerate 2-kinase	
H16_A36 02	K00873	4,82	pyruvate kinase [EC: <a href="#">2.7.1.40</a> ]   (GenBank) pyk2; pyruvate kinase	
H16_B01 79	No KO assigned	7,51	hemagglutinin-related transmembrane protein	No pathway
H16_B01 80	No KO assigned	7,37	hemagglutinin transmembrane protein	No pathway
H16_A27 77	K03782	2,49	catalase-peroxidase [EC:1.11.1.21]   (GenBank) katG	Amino Acid metabolism
H16_B10 00	K17285	2,28	methanethiol oxidase [EC:1.8.3.4]	
H16_B19 39	K00146	2,39	phenylacetaldehyde dehydrogenase [EC:1.2.1.39]   (GenBank) feaB	
H16_B22 34	K00167	3,11	2-oxoisovalerate dehydrogenase E1 component beta subunit [EC:1.2.4.4]	
H16_B22 35	K09699	3,64	2-oxoisovalerate dehydrogenase E2 component	

			(dihydrolipoyl transacylase) [EC:2.3.1.168]	
H16_B13 94	K01602	2,71	ribulose-bisphosphate carboxylase small chain [EC:4.1.1.39]   (GenBank) cbbS2	RuBiSCO assembly
H16_B13 95	K01601	2,85	ribulose-bisphosphate carboxylase large chain [EC:4.1.1.39]	
PHG426	3,15	K01602	ribulose-bisphosphate carboxylase small chain [EC:4.1.1.39]	
PHG427	2,86	K01601	ribulose-bisphosphate carboxylase large chain [EC:4.1.1.39]	
H16_B23 49	No KO assigned	2,24	response regulator-like protein containing sigma54 activator	Sigma factor activator
PHG064	K06282	2,71	hydrogenase small subunit [EC:1.12.99.6]	Hydrogenase complex
PHG065	K06281	2,72	hydrogenase large subunit [EC:1.12.99.6]	
PHG073	K04653	6,63	hydrogenase expression/formation protein HypC   (GenBank) hypC2; HypC2 hydrogenase	

			expression/formation protein HypC
PHG078	K04652	3,18	hydrogenase nickel incorporation protein HypB   (GenBank) hypB3; HypB3 hydrogenase nickel incorporation protein HypB

**Table E2.** Downregulated genes Adapted condition

Gene	KEGG code	Log2 Fold Change	Function	Pathway
H16_A3637	K02112	-2,18	F-type H <sup>+</sup> /Na <sup>+</sup> -transporting ATPase subunit beta [EC:7.1.2.2 7.2.2.1]	Oxidative phosphorylation
H16_A1055	K00335	-2,13	NADH-quinone oxidoreductase subunit F [EC:7.1.1.2]   (GenBank) nuoF	
H16_A1056	K00336	-2,22	NADH-quinone oxidoreductase subunit G [EC:7.1.1.2]   (GenBank) nuoG	
H16_A1057	K00337	-2,16	NADH-quinone oxidoreductase subunit H [EC:7.1.1.2]   (GenBank) nuoH	

H16_A105 9	K00339	-2,08	NADH-quinone oxidoreductase subunit J [EC:7.1.1.2]   (GenBank) nuoJ	
H16_A106 1	K00341	-2,18	NADH-quinone oxidoreductase subunit L [EC:7.1.1.2]   (GenBank) nuoL	
H16_A106 2	K00342	-2,30	NADH-quinone oxidoreductase subunit M [EC:7.1.1.2]   (GenBank) nuoM	
H16_A106 3	K00343	-2,39	NADH-quinone oxidoreductase subunit N [EC:7.1.1.2]   (GenBank) nuoN	
H16_A143 8	K00626	-2,13	acetyl-CoA C-acetyltransferase [EC:2.3.1.9]   (GenBank) phaA	PHA production
H16_A143 9	K00023	-2,73	acetoacetyl-CoA reductase [EC:1.1.1.36]   (GenBank) phaB1	

**Table E3.** Upregulated genes Not adapted condition

Gene	KEGG code	Log2 Fold	Function	Pathway
------	--------------	--------------	----------	---------

		Change		
H16_A2 172	No KO assigned	3,43	KO assigned (GenBank) phaP3; Phasin (PHA-granule associated protein)	PHA-granule associated protein
H16_A2 173	K17686	5,04	P-type Cu <sup>+</sup> transporter [EC:7.2.2.8] (GenBank) copF; copper efflux P-type ATPase	Mineral absorption
H16_A3 667	K19591	4,61	MerR family transcriptional regulator, copper efflux regulator (GenBank) cueR; transcriptional regulator	
H16_A3 668	K17686	4,47	P-type Cu <sup>+</sup> transporter [EC:7.2.2.8] (GenBank) copP2; putative copper uptake P-type ATPase	
H16_A3 665	No KO assigned	4,65	KO assigned (GenBank) h16_A3665;	No pathway

			transcriptional regulator, LysR-family	
H16_A3 666	K01048	4,85	lysophospholipase [EC:3.1.1.5]   (GenBank) pldB; Lysophospholipase	Glycerophospholipid metabolism